

co2amp 2020

Mikhail Polyanskiy

December 18, 2023

# Contents

<b>1</b>	<b>General notes</b>	<b>3</b>
1.1	Program Capabilities . . . . .	3
1.2	Availability, Tools, and Third Party Components . . . . .	4
1.3	Acknowledgements . . . . .	4
<b>2</b>	<b>Basic Concepts</b>	<b>5</b>
2.1	<code>co2amp</code> and <code>co2amp+</code> . . . . .	5
2.2	Projects . . . . .	5
2.3	Pulse, Layout and Optic . . . . .	5
2.4	Calculation Grid . . . . .	6
2.5	Units . . . . .	7
2.6	Program Output . . . . .	8
2.7	"Comments" and "About" Tabs of <code>co2amp+</code> . . . . .	8
<b>3</b>	<b>Elements of a Project</b>	<b>10</b>
3.1	Pulse . . . . .	10
3.2	Layout . . . . .	11
3.2.1	Configuration . . . . .	11
3.2.2	Dealing with Long Optical Elements . . . . .	11
3.2.3	Modeling of Pulse Propagation Between Optics . . . . .	12
3.3	Optic Type A: <i>Active Medium</i> . . . . .	14
3.4	Optic Type P: <i>Probe</i> . . . . .	15
3.5	Optic Type F: <i>Spatial Filter</i> . . . . .	15
3.6	Optic Type S: <i>Spectral Filter</i> . . . . .	15
3.7	Optic Type L: <i>Lens</i> . . . . .	16
3.8	Optic Type M: <i>Material</i> . . . . .	17
3.9	Optic Type C: <i>Chirper</i> . . . . .	18
<b>4</b>	<b>Modelling of processes in CO<sub>2</sub> amplifiers</b>	<b>19</b>
4.1	Molecular dynamics . . . . .	19
4.1.1	Pumping by electric discharge . . . . .	19
4.1.2	Pumping and vibrational relaxation dynamics . . . . .	20
4.1.3	Optical pumping . . . . .	21
4.2	Amplification . . . . .	22
4.2.1	Laser transitions . . . . .	22
4.2.2	Main equations . . . . .	22
4.2.3	Populations . . . . .	24
	<b>Appendices</b>	<b>26</b>

A Cross-sections of excitation processes	27
B Molecular constants	31
C Properties of optical materials	39
D Selected formulas explained	42

# Chapter 1

## General notes

### 1.1 Program Capabilities

1. Ultrashort pulse amplification in CO<sub>2</sub> active medium
  - Rotational numbers up to  $J = 60$
  - Regular, hot, and sequence bands
  - Isotopic CO<sub>2</sub>
2. Molecular dynamics
  - Realistic pumping
  - Collisional relaxation processes
  - Stimulated transitions
  - Independent consideration of active medium regions at different elongations from the optical axis
3. Diffraction-based beam propagation
  - Beam manipulation with common optical elements
  - Arbitrary optical configurations
4. Linear dispersion and non-linear effects in optical materials
  - Pulse chirping
  - Kerr lensing
  - Self-phase modulation
5. Advanced optics
  - Chirped-pulse amplification
  - Spectral filtering
  - Trains of pulses
  - Staging (program output as an input for the next stage)
6. User's interface
  - Easy specification of parameters
  - Graphical output
  - Project save/recall

## 1.2 Availability, Tools, and Third Party Components

The simulation core **co2amp** and the user's interface shell **co2amp+** are written in the C++ programming language. **co2amp+** utilizes the QT library (<http://qt.io>), and QT Creator, a component of the QT project, is employed as the development environment. Windows executables are compiled using the MinGW compiler, which is part of the open-source QT distribution. The code is hosted on GitHub (<https://github.com/polyanskiy/co2amp>) and is freely available for use, modification, and redistribution under the GNU General Public License (GPL v.3) (<https://www.gnu.org/licenses/gpl-3.0.html>). A binary package is available as a Windows installer, containing pre-compiled executables, documentation, templates, and examples at <https://github.com/polyanskiy/co2amp/releases/>. The project leverages cross-platform libraries, facilitating compilation on other platforms (MacOS, Linux). **co2amp** relies on three third-party components: gnuplot, 7-zip, and HDF5, available at <http://www.gnuplot.info/>, <https://www.7-zip.org/>, and <https://www.hdfgroup.org/solutions/hdf5/>, respectively. These components must be installed separately. The Windows installer is created using the Nullsoft Scriptable Install System (NSIS, <https://nsis.sourceforge.io/>), representing the only platform-specific component of the project. The documentation is primarily written in L<sup>A</sup>T<sub>E</sub>X (<http://www.latex-project.org>) using the Overleaf online editor and compiler (<https://www.overleaf.com/>). YAML and HDF5 file formats are adopted for specifying input parameters and storing output field information, respectively.

## 1.3 Acknowledgements

Viktor Platonenko from Moscow State University (Russia) provided a Mathcad code for pulse amplification in the CO<sub>2</sub> active medium, which served as the starting point for developing the **co2amp** program. Dr. Platonenko also offered valuable input during the early stages of the work on **co2amp+**.

# Chapter 2

## Basic Concepts

### 2.1 `co2amp` and `co2amp+`

`co2amp` is a terminal program designed for simulating the propagation of ultrashort pulses through an arbitrary cylindrically-symmetric optical system, which may include CO<sub>2</sub> amplifiers. It operates using inputs in the form of specially formatted text files and command line arguments, and generates outputs as tabulated data files and a binary file containing comprehensive information on the output field. While `co2amp` can function independently, its use is greatly facilitated by a graphical user interface, which significantly simplifies the management of the program's inputs and outputs.

`co2amp+` is a graphical user interface program that streamlines the process of handling multiple input and output files, as well as calculation parameters, by maintaining an organized and easily navigable working environment. `co2amp+` features functionality for saving and recalling the entire file structure of a project along with command line parameters in a single compressed '.co2' file.

### 2.2 Projects

The `co2amp` input parameters include the characteristics of the initial `pulse(s)`, the optical `layout` configuration, specifications for all `optics` used in the model (including laser amplifiers), and calculation parameters (e.g., calculation grid definition).

The temporal shape of the pulse and the beam profile at every element of the optical layout are saved and can be accessed in both graphical and tabulated-numerical representations.

All `co2amp` inputs and outputs for a certain model constitute a project.

`co2amp+` facilitates the storage of all inputs and outputs of the model, except for the output field, in a single compressed project file with a '.co2' extension. Complete pulse information (complex field at every node of the space-time calculation grid) at the system's output can be saved separately as a binary HDF5 file (with a '.pulse' extension) and used as an input for another project. An example of the input file structure of a '.co2' project accessed via the `co2amp+` interface is illustrated in Fig. 2.1.

### 2.3 Pulse, Layout and Optic

A `pulse` is a complex electric field defined at every node of the calculation grid. A project can include one or more input pulses. Each is defined in a separate YAML ('.yaml') file. A pulse can be defined either by referencing an output from another project (a '.pulse' file) or by explicitly specifying the pulse's spatial and temporal profile.

The optical `layout` consists of a series of infinitely-thin `optics` separated by free space. `Pulses` propagate freely between `optics`. A project must have exactly one `layout`. The `layout` is defined in a '.yaml' file that

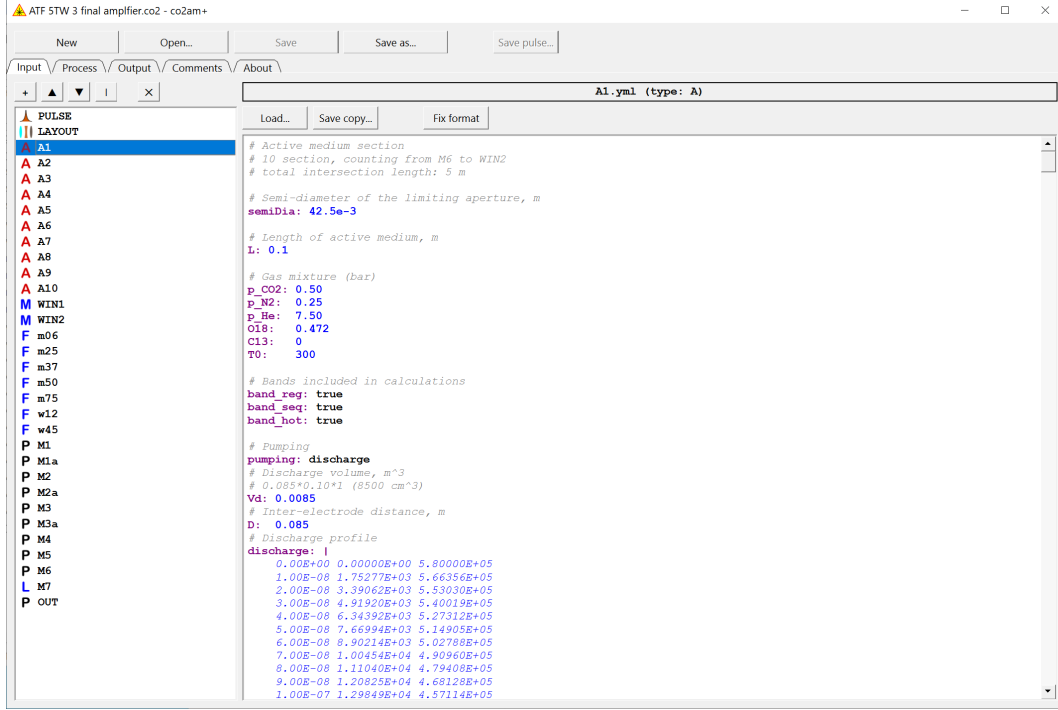


Figure 2.1: "Input" tab of the **co2amp+** user interface program. YAML files specifying the pulse, layout, and optics are listed on the left. Content of a selected file is displayed and can be edited in the big edit box on the right.

specifies the order of the **planes** and the distances between them.

An **optic** is a system element that alters the pulse as it passes through. Several types of **optics** are described in detail later. For example, a *Lens* is an **optic** introducing a radial-coordinate-dependent frequency shift, altering the beam's divergence. Each **optic** is specified in a separate '.yaml' file. An **optic** can be used multiple times in the same **layout**, as in a laser cavity<sup>1</sup>.

**co2amp** supports seven types of **optics**, listed in Table 2.1.

## 2.4 Calculation Grid

The **pulse** is defined as a complex electric field at the nodes of a 2-dimensional space-time calculation grid, which moves with the pulse. The calculation grid is primarily defined via **co2amp** command line arguments. The only exception is the maximum radial coordinate, equal to the semi-diameter of the clear aperture of an **optic**, and thus varies from one **optic** to another. The command line arguments associated with the pulse's space-time calculation grid include the numbers of nodes (representing "precision") in the time and radial coordinate grids, the minimum and maximum time limits, and the central frequency. The central frequency is essential for unambiguously defining the calculation grid in the frequency domain.

The pulse time frame is utilized for all **pulse**-related calculations (interaction with **optics**, free-space propagation) and for fast processes in some **optics**, such as fast molecular dynamics (stimulated transitions and rotational relaxation in an *Active Medium*). Processes significantly slower than the pulse duration (like

<sup>1</sup>Internally, the **co2amp** code employs an additional concept: a **plane**. A **plane** is a **layout** element that, unlike an **optic**, appears in the **layout** only once. An **optic** is then associated with each **plane**. Essentially, a **plane** is a placeholder for an **optic**.

Table 2.1: Types of Optics

<i>Type ID</i>	<i>Name</i>	<i>Description</i>
A	<i>Active medium</i>	A CO <sub>2</sub> amplifier section.
P	<i>Probe</i>	A passive surface. May be used as a limiting aperture.
F	<i>Spatial filter</i>	An optic with coordinate-dependent transmission.
S	<i>Spectral filter</i>	An optic with frequency-dependent transmission.
L	<i>Lens</i>	An ideal thin lens.
M	<i>Material</i>	A layer of material. May introduce linear and/or non-linear dispersion and/or absorption.
C	<i>Chirper</i>	An optic that applies a chirp to the pulse. Typically a stretcher or compressor.

the pumping of the active medium and vibrational relaxation) are modeled separately in a slower laboratory time-frame. The time-tick of this laboratory time-frame is also defined via a **co2amp** command line argument.

In **co2amp+**, the **co2amp** command line arguments are specified in the "Process" tab (Fig. 2.2). The number of nodes in both coordinates of the pulse space-time frame is always a power of two, enabling the use of Fast Fourier Transform (FFT) algorithms. Calculations with more nodes are generally more accurate but require longer computation times and more computer memory (both calculation time and required memory are approximately proportional to the product of the number of nodes in the time and space grids). Therefore, it is recommended to start the simulation with a smaller number of nodes and incrementally increase the grid density, repeating the simulation multiple times. The absence of significant changes in the program's output with an increase in the number of nodes indicates that the grid density is satisfactory.

The time-step,  $\Delta t = (t_{\max} - t_{\min})/N_t$ , where  $t_{\max}$  and  $t_{\min}$  define the time range and  $N_t$  is the number of nodes in the time grid, must be sufficiently small to accurately describe the pulse profile throughout its propagation in the optical system. It is also important to note that the time range and the number of nodes in the time grid define the frequency domain range and step:  $\Delta\nu = 1/(t_{\max} - t_{\min})$  and  $(\nu_{\max} - \nu_{\min}) = 1/\Delta t$ . This means that the time range must be long enough to provide adequate resolution in the frequency domain, while the time step must be short enough to encompass the entire spectral region of interest.

Identifying an appropriate calculation grid is crucial for building an accurate model of an optical system. Investing effort in this part of the simulation process will yield fast and reliable calculations.

## 2.5 Units

SI units without prefixes, such as "meters, seconds, Amperes" (but not "centimeters, nanoseconds, kiloamperes"), are used in **co2amp** for input, output, and also internally within the code. **co2amp+** provides the functionality to change the units used for graphical representation of the calculation results on the "Output" tab (Fig. 2.3). However, when numerical data are accessed via [Right-click on a plot] – [Copy raw data], the units of the data are always in their "prefix-less" form.



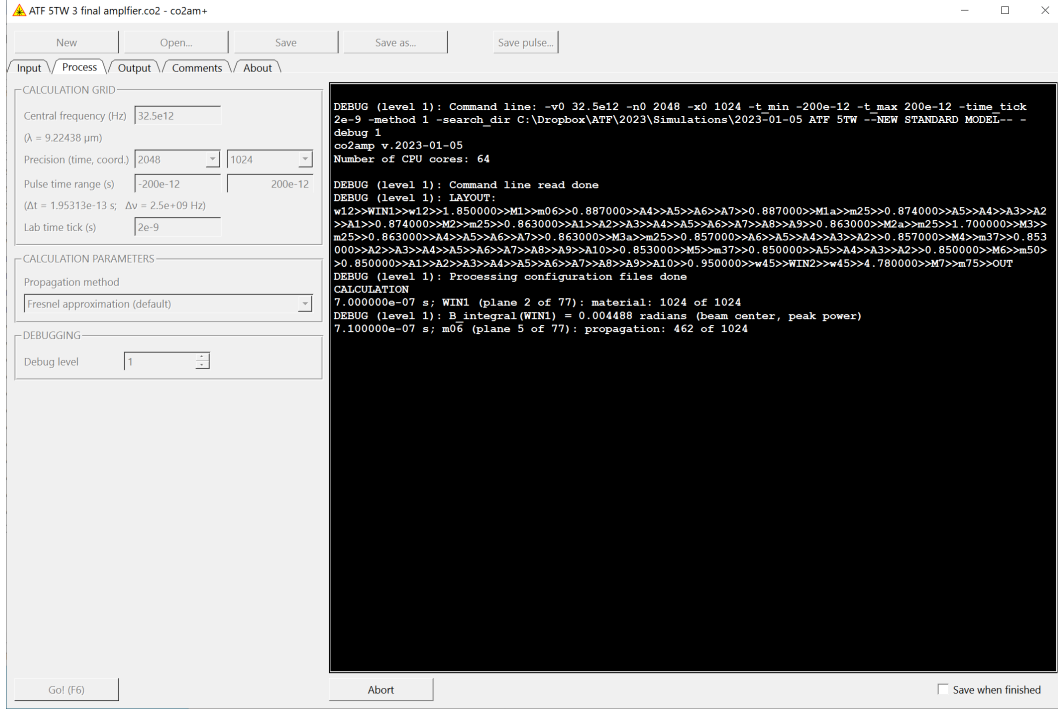


Figure 2.2: "Process" tab of the **co2amp+** user interface program. Values of **co2amp** command line arguments are specified on the left. **co2amp** output is displayed in the black text box on the right.

## 2.6 Program Output

The output of the program includes the temporal and spatial structure of each **pulse** at every **optic** within the **layout**. Temporal (and spectral) profiles are integrated over the entire area of the **optic**, while spatial profiles are integrated over the duration of the pulse time-frame.

In the **co2amp+** "Output" tab, users can choose a **pulse** and an **optic** to display (Fig. 2.3). If the selected **optic** is utilized multiple times in the **layout**, there is also an option to specify which passes through the **optic** are to be displayed. Additionally, the integral pulse energy can be provided either at each pass through a selected **optic** or across all passes through all **optics** in the **layout**.

Output for certain types of **optics** includes additional type-specific information. For example, for an *Active medium*, this encompasses gain, discharge profile, population dynamics, and the dynamics of the distribution of pumping energy (fractions of discharge energy contributing to the excitation of laser levels, excitation of molecular translations, and ionization). Output for an **optic** of type *Probe* includes information on the phase of the optical field at the center of the beam.

## 2.7 "Comments" and "About" Tabs of co2amp+

The "Comments" tab in **co2amp+** provides an editable text box where users can enter any comments about the project. These comments will be stored as part of the project in the '.co2' file.

The "About" tab contains information about the versions of **co2amp** and **co2amp+**, including links to the license and the documentation (this file), author contact information, and a suggested citation format.

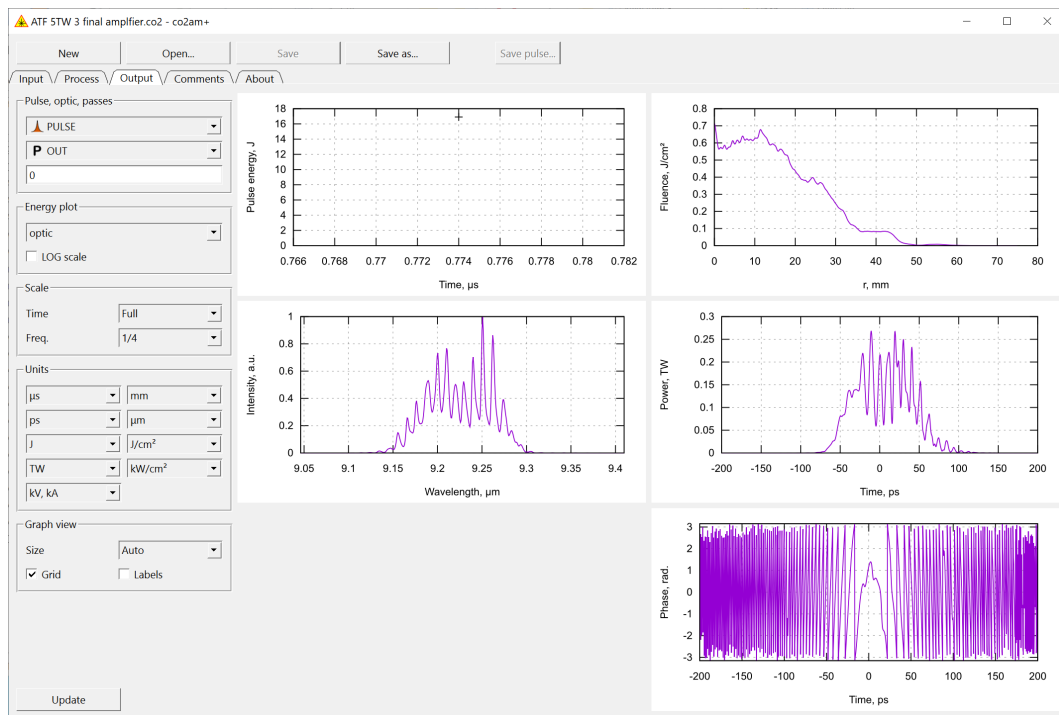


Figure 2.3: "Output" tab of the **co2amp+** user interface program. Controls on the left allow selecting the data to display and fine-tuning the look of the plots.

# Chapter 3

## Elements of a Project

A project in **co2amp** must include the following elements, each specified in separate input YAML (’.yaml’) files:

1. One or more **pulses**
2. One or more **optics**
3. One **layout**

Each element is detailed in its dedicated YAML file<sup>1</sup>. The last **optic** in the **layout** must be of type **P** (*Probe*).

The subsequent sections provide brief descriptions of each of these elements and the models associated with them. For a comprehensive understanding, refer to the templates, example files, and the comments within them.

### 3.1 Pulse

Unless utilizing the output of another project (a ’pulse’ file) as input, both the temporal and spatial shape of the input **pulse** must be defined in a corresponding YAML (’.yaml’) file. The **pulse** is assumed to be transform-limited, meaning it has no initial chirping. Specifications such as the **pulse** energy, central frequency, and injection time are also required. The injection time denotes the time-delay between the zero moment of the laboratory time frame (”slow” time frame) and the injection of a **pulse** into the optical system (the first **optic** in the **layout**). An example of a **pulse** configuration file is provided below.

```
#=====
# PULSE.yaml from 'examples/00 simple propagation.co2' project

t_in: 0
E: 1e-3
freq: 32.5e12

beam: GAUSS
w: 3e-3

pulse: GAUSS
fwhm: 2e-12
```

---

<sup>1</sup>**co2amp** additionally requires an input file ’config\_files.yaml’ that enumerates all input YAML files and the types of corresponding elements. **co2amp+** automatically generates this file.

```
#=====
```

This file specifies a 2 ps (FWHM) transform-limited Gaussian pulse with a  $w = 3$  mm Gaussian beam profile, 1 mJ energy, and a 32.5 THz central frequency, injected into the system at  $t_{\text{in}} = 0$ . Several pre-defined beam and pulse profile options are available, such as **GAUSS**, **FLATTOP**, **SUPERGAUSS4**, **SUPERGAUSS6**, etc. Alternatively, a **FREEFORM** option allows for the specification of an arbitrary shape through a tabulated numerical profile (refer to the 'pulse.yml' template for details).

## 3.2 Layout

### 3.2.1 Configuration

The **layout** configuration defines the sequence of **optics** and the distances between them in the optical system. Below is an example of a simple **layout** configuration file:

```
#=====
# LAYOUT.yml from 'examples/00 simple propagation.co2' project

- go: P1 >> 3 >> P2
  times: 1
#=====
```

In this example, the system consists of two **optics**, P1 and P2, separated by 3 meters of free space. The pulses pass through the system once. If the **times** value is greater than 1, a pulse after passing through P2 will return to P1, and the propagation through the system will repeat for the specified number of times. A **layout** configuration file can contain several such "go-times" sequences. Below is an example of a **layout** configuration for a more complex system:

```
#=====
# LAYOUT.yml from 'examples/ATF 5 TW/ATF 1 regen.co2' project

- go: str >> COU1
  times: 1

- go: 0.45 >> i >> 0.90 >> GE >> 0.25 >> w >> WIN1 >> w >> 0.45 >> AM1 >> 0.40 >> AM2 >> 0.45
>> w >> WIN2 >> w >> 0.10 >> MIR >> m >> 0.10 >> w >> WIN2 >> w >> 0.45 >> AM2 >> 0.40 >> AM1
>> 0.45 >> w >> WIN1 >> w >> 0.25 >> GE >> 0.90 >> i >> 0.45 >> COU2
  times: 15

- go: 0.45 >> i >> 0.90 >> GE >> 0.25 >> w >> WIN1 >> w >> 0.45 >> AM1 >> 0.40 >> AM2 >> 0.45
>> w >> WIN2 >> w >> 0.10 >> MIR >> m >> 0.10 >> w >> WIN2 >> w >> 0.45 >> AM2 >> 0.40 >> AM1
>> 0.45 >> w >> WIN1 >> w >> 0.25 >> OUT
  times: 1
#=====
```

### 3.2.2 Dealing with Long Optical Elements

In the **co2amp** model, **optics** are considered infinitely thin. For long **optics**, such as an *Active Medium*, the model calculates the field modification accumulated by a **pulse** as it propagates through the **optic** and then applies this modification as if it occurred instantaneously. However, this approach might not be accurate if the actual optical element is lengthy and the **pulse** changes significantly while propagating through it, thereby interacting differently with various parts of the **optic**. The model's accuracy can be improved by dividing long elements into shorter sub-sections.

Fig. 3.1 illustrates an example of a 2-meter long layout with a meter-long active medium in the middle. In one scenario, shown in Fig. 3.1a, we first propagate the pulse to the midpoint of the amplifier section, then apply the amplification accumulated over 1 meter, and finally propagate the pulse to the last optic. The corresponding layout configuration is:

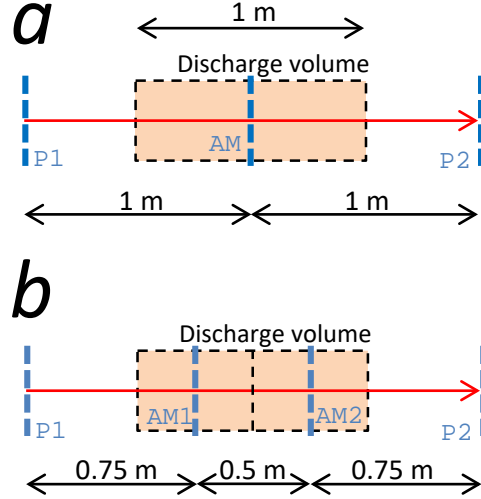


Figure 3.1: Example of layout configuration for a long optic (in this case, an *Active Medium*). a) The *Active Medium* is represented by a single optic. b) The *Active Medium* is split into two shorter sections.

```
#=====
# long amplifier

- go: P1 >> 1 >> AM >> 1 >> P2
  times: 1
#=====
```

Alternatively, the active medium can be represented by two 0.5-meter sections, as shown in Fig. 3.1b. The corresponding layout is:

```
#=====
# long amplifier divided into two shorter sections

- go: P1 >> 0.75 >> AM1 >> 0.5 >> AM2 >> 0.75 >> P2
  times: 1
#=====
```

By splitting a long amplifier into shorter sections, the population dynamics within each amplifier section is modeled more accurately, leading to a more realistic representation of the active medium.

### 3.2.3 Modeling of Pulse Propagation Between Optics

Consider free-space wave propagation between plane-parallel surfaces  $S'$  and  $S$ , separated by distance  $z$ , as illustrated in Fig. 3.2 for a system with cylindrical symmetry. According to the Huygens-Fresnel principle, the field  $E$  at a point on plane  $S$  is defined as a superposition of secondary waves emitted from every point

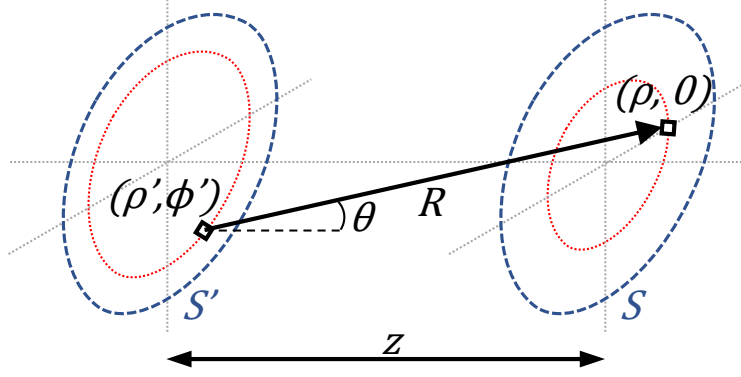


Figure 3.2: Application of the Huygens-Fresnel principle to beam propagation from plane  $S'$  to plane  $S$  in a system with cylindrical symmetry.

of plane  $S'$  [1]. This can be expressed in the case of cylindrical symmetry as [2, 3]:

$$E(\rho) = -\frac{i}{\lambda} \int_{\rho'=0}^{\infty} E'(\rho') \int_{\phi'=0}^{2\pi} \frac{e^{ikR}}{R} K d\phi' \rho' d\rho' \quad (3.1a)$$

$$R = \sqrt{\rho^2 + \rho'^2 + z^2 - 2\rho\rho' \cos \phi'} \quad (3.1b)$$

$$K = \cos \theta = \frac{z}{R} \quad (3.1c)$$

where  $\lambda$  is the wavelength,  $k = 2\pi/\lambda$  the wavenumber, and  $K$  the obliquity factor as it appears in Rayleigh-Sommerfeld diffraction theory.

Since the field on the output plane  $S$  does not depend on the angular coordinate  $\phi$ ,  $\phi = 0$  is chosen for the simplification of Eq. 3.1.

Direct numerical integration of Eq. 3.1, with  $O(N^3)$  complexity, is very time-consuming. Therefore, an approximation is usually employed to accelerate computations. The most well-known approximation is Fresnel diffraction, which assumes:

$$K \approx 1$$

$$R \approx \begin{cases} z & \text{(denominator)} \\ z \left( 1 + \frac{\rho^2 + \rho'^2 - 2\rho\rho' \cos \phi'}{2z^2} \right) & \text{(exponent)} \end{cases} \quad (3.2)$$

where "denominator" and "exponent" indicate the position of the  $R$  variable in Eq. 3.1a.

Substituting Eq. 3.2 into Eq. 3.1a and using the formula

$$\int_0^{2\pi} e^{\pm ia \cos \phi} d\phi = 2\pi J_0(a) \quad (3.3)$$

where  $J$  is the Bessel function, we obtain the expression for Fresnel diffraction with cylindrical symmetry:

$$E(\rho) \approx -\frac{2\pi i e^{ik\left(z + \frac{k\rho^2}{2z}\right)}}{\lambda z} \int_0^{\infty} E'(\rho') e^{i\frac{k\rho'^2}{2z}} J_0\left(\frac{k\rho\rho'}{z}\right) \rho' d\rho' \quad (3.4)$$

**co2amp** supports both Rayleigh-Sommerfeld (Eq. 3.1) and Fresnel (Eq. 3.4) based propagation methods. Users can also choose to ignore the **pulse** evolution during free-space propagation.

Eqs. 3.1 and 3.4 assume monochromatic light, which is not the case for ultrashort pulses that possess a non-negligible bandwidth. Therefore, in **co2amp**, propagation is calculated in the frequency domain: Eqs. 3.1 or 3.4 are applied to the Fourier-transformed field at each node of the frequency calculation grid. Afterward, an inverse Fourier transform is used to return to the time domain.

### 3.3 Optic Type A: *Active Medium*

The *Active Medium* is the most complex type of **optic** that can be utilized in a **co2amp** project. Detailed models used for simulating molecular dynamics and **pulse** amplification are described in a dedicated Chapter 4.

A configuration file for an **optic** of type A must include specifications of the gas mixture, pumping mechanism, and laser transitions considered in the simulations. An example of such a configuration file is provided below:

```
#=====
# AM1.yml from 'examples/ATF 5 TW/ATF 3 final amplifier.co2' project

# Semi-diameter of the limiting aperture, m
semiDia: 45e-3

# Length of active medium, m
L: 0.57

# Gas mixture (bar)
p_CO2: 0.50
p_N2: 0.25
p_He: 7.50
O18: 0.472
C13: 0
T0: 300

# Bands included in calculations
band_reg: true
band_seq: true
band_hot: true

# Pumping
pumping: discharge
# Discharge volume, m^3
Vd: 0.0085
# Inter-electrode distance, m
D: 0.085
# Discharge profile
discharge: |
    0.00E+00 0.00000E+00 5.80000E+05
    1.00E-08 1.97186E+03 5.66356E+05
    2.00E-08 3.81445E+03 5.53030E+05
    3.00E-08 5.53410E+03 5.40019E+05
    4.00E-08 7.13691E+03 5.27312E+05
    ...
#=====
```

The composition of the active medium, including isotopic enrichment of carbon dioxide, and the initial temperature are specified under the "Gas mixture (bar)" section.

For discharge pumping, the geometry of the discharge and its temporal profile are required. In the case of optical pumping, the wavelength, absorption cross-section, and the temporal profile of the pumping pulse must be provided.

The 'optic A (discharge pumped CO2 amplifier).yaml' and 'optic A (optically pumped CO2 amplifier).yaml' template files contain detailed information on the configuration file format and can be referred to for further guidance.

### 3.4 Optic Type P: *Probe*

A *Probe* is a passive type of **optic**. It does not alter the field that fits within its semi-diameter. This can be expressed mathematically as:

$$E(t, \rho) = E'(t, \rho) \quad (3.5)$$

where  $E'(t, \rho)$  and  $E(t, \rho)$  represent the field before and after passing through an **optic**, respectively.

However, a *Probe* **optic** can serve as a limiting aperture, exhibiting zero transmittance for  $\rho > \text{semiDia}$ . The sole configuration parameter for an **optic** of type P is its semi-diameter. An example of a configuration file for a *Probe* with a 25 mm semi-diameter is shown below:

```
#####
# probe

semiDia: 25e-3
#####
```

### 3.5 Optic Type F: *Spatial Filter*

A *Spatial Filter* applies a specified coordinate-dependent transmittance function to a **pulse**:

$$E(t, \rho) = E'(t, \rho) \sqrt{\mathcal{T}(\rho)} \quad (3.6)$$

where  $\mathcal{T}(\rho)$  is the transmittance function, as defined in the configuration file.

An example configuration for a *Spatial Filter* is shown below:

```
#####
# spatial filter

semiDia: 25e-3

filter: SIN
r_min: 10e-3
#####
```

For more details and configuration options, refer to the 'optic F (spatial filter).yaml' template file.

### 3.6 Optic Type S: *Spectral Filter*

A *Spectral Filter* applies a specified frequency-dependent transmittance function to a **pulse**:



$$\begin{aligned}
\hat{E}'(\nu, \rho) &= \mathcal{F}(E'(t, \rho)) \\
\hat{E}(\nu, \rho) &= \hat{E}'(\nu, \rho) \sqrt{\mathcal{T}(\nu)} \\
E(t, \rho) &= \mathcal{F}^{-1}(\hat{E}(\nu, \rho))
\end{aligned} \tag{3.7}$$

where  $\mathcal{F}$  and  $\mathcal{F}^{-1}$  denote the Fourier transform and the inverse Fourier transform, respectively,  $\nu$  is the frequency, and  $\mathcal{T}(\nu)$  is the transmittance function as defined in the configuration file.

An example configuration for a *Spectral Filter* is provided below:

```

#=====
# spectral filter

semiDia: 25e-3

filter: FREEFORM
form: |
    32.0e12 1.0
    32.1e12 0.9
    32.2e12 0.7
    32.3e12 0.5
    32.4e12 0.3
    32.5e12 0.0
    32.6e12 0.3
    32.7e12 0.5
    32.8e12 0.7
    32.9e12 0.9
    33.0e12 1.0
#=====

```

For further details and configuration options, refer to the 'optic S (spectral filter).yml' template file.

### 3.7 Optic Type L: *Lens*

A *Lens* functions as a standard optical lens within the system:

$$\begin{aligned}
\hat{E}'(\nu, \rho) &= \mathcal{F}(E'(t, \rho)) \\
\hat{E}(\nu, \rho) &= \hat{E}'(\nu, \rho) \exp\left(-\frac{ik\rho^2}{2F}\right) \\
E(t, \rho) &= \mathcal{F}^{-1}(\hat{E}(\nu, \rho))
\end{aligned} \tag{3.8}$$

where  $k = \frac{2\pi\nu}{c}$  is the wave number ( $c$  is the speed of light) and  $F$  is the focal length of the lens.

The calculation is performed in the frequency domain to ensure that the effective focal length remains consistent across all frequencies in the pulse spectrum.

An example configuration for a lens with a 1-meter focal length is shown below:

```

#=====
# lens (F = 1 m)

semiDia: 25e-3

F: 1.0
#=====

```

### 3.8 Optic Type M: *Material*

In cases of oblique incidence, the effective intensity  $I_{\text{eff}}$  is reduced and the propagation distance in the material (effective thickness)  $\Theta_{\text{eff}}$  is automatically adjusted based on the incidence angle  $\theta_i$  and the refractive index  $n$ :

$$\begin{aligned}\theta_r &= \arcsin\left(\frac{\sin \theta_i}{n_0}\right) \\ I_{\text{eff}} &= I \frac{\cos \theta_i}{\cos \theta_r} \\ \Theta_{\text{eff}} &= \frac{\Theta}{\cos \theta_r}\end{aligned}\tag{3.9}$$

where  $I$  and  $\Theta$  are the intensity before the **optic** and the actual thickness of the material, respectively, and  $\theta_r$  is the refraction angle.

#### Linear Dispersion and Absorption

$$\begin{aligned}\hat{E}'(\nu, \rho) &= \mathcal{F}(E'(t, \rho)) \\ \hat{E}(\nu, \rho) &= \hat{E}'(\nu, \rho) \exp(2\pi i \Delta\nu) \sqrt{\exp(-\alpha_0 \Theta_{\text{eff}})} \\ E(t, \rho) &= \mathcal{F}^{-1}(\hat{E}(\nu, \rho))\end{aligned}\tag{3.10}$$

where  $\Delta\nu$  is defined as:

$$\Delta\nu = \int_0^\nu (\nu' - \nu_c) \frac{dt}{d\nu'} d\nu',\tag{3.11}$$

$$\frac{dt}{d\nu'} = \frac{\Theta_{\text{eff}}}{c} \frac{dn_g}{d\nu'},\tag{3.12}$$

with  $c$  as the speed of light,  $n_g$  as the group index of refraction, and  $\nu_c$  as the central frequency. The dispersion formulas used for calculating  $n_g$  are given in Appendix C.

#### Nonlinear Interaction

$$\begin{aligned}E(t, \rho) &= E'(t, \rho) \exp\left(2\pi i \nu_c \frac{\Theta_{\text{eff}}}{c} n_2 I_{\text{eff}}(t, \rho)\right) \\ I_{\text{eff}}(t, \rho) &= 2h\nu_c (E'(t, \rho))^2 \frac{\cos \theta_i}{\cos \theta_r}\end{aligned}\tag{3.13}$$

where  $n_2$  is the nonlinear refractive index,  $h$  is Planck's constant, and  $I(t, r)$  is the field intensity. Numerical values of  $n_2$  used in the program are given in Appendix C.

Configuration example for a *Material optic*:

```
#=====
# material

semiDia: 25e-3

material: NaCl
thickness: 100e-3
tilt: 0
slices: 10
#=====
```

Currently supported materials include AgBr, AgCl, BaF<sub>2</sub>, CdTe, CsI, GaAs, Ge, IRG22 (AMTIR1), IRG24, IRG25, KBr, KCl, KRS5, NaCl, NaF, Si, SiO<sub>2</sub>, ZnS, ZnSe, and air. An arbitrary  $n_2$  can be specified in the configuration file, with a predefined value used otherwise (see Appendix C). To enhance accuracy, the *Material optic* can be divided into several layers. A split-step method is employed for calculating linear and nonlinear interactions with a layer: first, a nonlinear interaction with a half-layer is calculated, followed by a full-layer linear interaction, and then a half-layer nonlinear interaction again.

### 3.9 Optic Type C: *Chirper*

A *Chirper* introduces a chirp to a pulse and is typically used to model a stretcher or compressor.

$$\begin{aligned}\widehat{E}'(\nu, \rho) &= \mathcal{F}(E'(t, \rho)) \\ \widehat{E}(\nu, \rho) &= \widehat{E}'(\nu, \rho) \exp(2\pi i \Delta\nu) \\ E(t, \rho) &= \mathcal{F}^{-1}(\widehat{E}(\nu, \rho))\end{aligned}\tag{3.14}$$

where

$$\Delta\nu = \int_0^\nu (\nu' - \nu_c) \frac{dt}{d\nu'} d\nu',\tag{3.15}$$

$\nu_c$  is the central frequency, and  $\frac{d\nu}{dt}$  is the chirpiness.

In the case of linear chirp, the chirpiness is constant, and Eq. 3.15 simplifies to:

$$\begin{aligned}\Delta\nu &= \int_0^\nu \frac{\nu' - \nu_c}{\mathcal{C}} d\nu' = \frac{(\nu - \nu_c)^2}{2\mathcal{C}} \\ \mathcal{C} &= \frac{d\nu}{dt}\end{aligned}\tag{3.16}$$

An example configuration for a *Chirper* with linear chirp is shown below:

```
#####
# stretcher (positive chirpiness => red chirp)

semiDia: 25e-3

chirp: LINEAR
c: 3.5e21
#####
```

Currently, only linear chirp is supported in the program.

## Chapter 4

# Modelling of processes in CO<sub>2</sub> amplifiers

### 4.1 Molecular dynamics

Simulations of active medium pumping by electric discharge and vibrational relaxation are done following Karlov and Konev [4].

#### 4.1.1 Pumping by electric discharge

Pumping is described by the Boltzmann equation in the following form [5, 6]:

$$\begin{aligned} -\frac{1}{3} \left( \frac{\mathcal{E}}{\mathcal{N}} \right)^2 \frac{d}{du} \left[ u \left( \sum_j y_j Q_{mj}(u) \right)^{-1} \frac{df(u)}{du} \right] = \\ 1.09 \times 10^{-3} \frac{d}{du} \left[ u^2 f(u) \sum_j \frac{y_j}{M_j} Q_{mj}(u) \right] + \sum_{j=1,2} y_j C_j \frac{d}{du} (u f(u)) + 6B y_2 \frac{d}{du} (u Q(u) f) \\ + \sum_j y_j \sum_k (u + u_{jk}) Q_{jk}(u + u_{jk}) f(u + u_{jk}) - u f(u) \sum_j y_j \sum_k Q_{jk}(u) \end{aligned} \quad (4.1)$$

where the left part describes the energy of electrons in the electric field, the first component of the sum of the right part represents energy transfer via elastic collisions between electrons and molecules, the second and third components describe collisions with molecular rotation excitation, and the two last components relate to inelastic collisions with transfer of the energy  $u_{jk}$  into vibrational and electronic excitations and ionization.

Electron energy  $u$  is expressed in eV;

Ratio of the electric field to the full molecular density,  $\mathcal{E}/\mathcal{N}$ , is expressed in units of  $10^{-16} \text{ V} \cdot \text{cm}^2$ ;

$y_j$  are the relative molecule concentrations ( $j = 1$  corresponds to CO<sub>2</sub>,  $j = 2$  to N<sub>2</sub> and  $j = 3$  to He);

$M_1 = 44$ ,  $M_2 = 28$ ,  $M_3 = 4$  are the molar masses;

$C_1 = 8.2 \times 10^{-4} \text{ eV} \cdot \text{\AA}^2$  [7];

$C_2 = 5.06 \times 10^{-4} \text{ eV} \cdot \text{\AA}^2$  [8];

$B = 2.5 \times 10^{-4} \text{ eV}$  is the N<sub>2</sub> rotational constant.

Numerical values of the cross-sections  $Q$  and the transferred energies  $u_{jk}$  are summarized in Appendix A

Equation 4.1 is solved numerically using the tridiagonal matrix algorithm. Distribution function  $f(u)$  is then used in the following calculations.

The rate constant  $\omega_{jk}$ , and the electron drift speeds  $v_d$  are defined as:

$$\omega_{jk} \left[ \frac{\text{cm}^3}{\text{s}} \right] = 5.93 \times 10^{-9} \int_0^\infty u Q_{jk}(u) f(u) du \quad (4.2)$$

$$v_d \left[ \frac{\text{cm}}{\text{s}} \right] = -5.93 \times 10^7 \left( \frac{1}{3} \frac{\mathcal{E}}{\mathcal{N}} \right) \frac{df(u)}{du} \int_0^\infty u \left( \sum_j y_j Q_{mj}(u) \right)^{-1} du \quad (4.3)$$

The fraction of electron energy transmitted via inelastic processes is defined as

$$z_{jk} = 10^{16} \frac{y_j u_{jk} \omega_{jk}}{\left( \frac{\mathcal{E}}{\mathcal{N}} \right) v_d} \quad (4.4)$$

The fraction of electron energy transmitted to translations and rotations are the following:

$$z_t = 5.93 \times 10^7 \frac{1.09 \times 10^{-3} \int_0^\infty u^2 \left( \sum_j \frac{y_j}{M_j} Q_{mj}(u) \right) f(u) du}{\left( \frac{\mathcal{E}}{\mathcal{N}} \right) v_d} \quad (4.5)$$

$$z_r = 5.93 \times 10^7 \frac{\sum_{j=1,2} y_j C_j \int_0^\infty u f(u) du + 6 y_2 B \int_0^\infty u Q(u) f(u) du}{\left( \frac{\mathcal{E}}{\mathcal{N}} \right) v_d} \quad (4.6)$$

Finally, the distribution of the excitation energy is calculated using the following expressions:

$$\begin{aligned} q_2 &= \sum_{k=1}^6 z_{1k} - \text{fraction of energy transferred to CO}_2 \text{ symmetric stretch } (\nu_1) \text{ and bending } (\nu_2) \text{ modes;} \\ q_3 &= z_{17} - \text{fraction of energy transferred to CO}_2 \text{ asymmetric stretch mode } (\nu_3); \\ q_4 &= \sum_{k=1}^8 z_{2k} - \text{fraction of energy transferred to N}_2 \text{ vibrations;} \\ q_T &= z_t + z_r - \text{fraction of energy transferred to translation and rotation;} \\ q_{ei} &= \sum_{k=9}^{15} z_{2k} + \sum_{k=8}^{10} z_{1k} - \text{fraction of energy spent on excitation of electronic levels and ionization.} \end{aligned}$$

#### 4.1.2 Pumping and vibrational relaxation dynamics

A 3-temperature model is used for describing the vibrational dynamics of the active medium of CO<sub>2</sub> amplifiers. In this model, the following temperatures are used to describe the distribution of the energy between molecular vibrations:

- $T_2$  – vibrational temperature of  $\nu_1$  and  $\nu_2$  vibrations of CO<sub>2</sub>;
- $T_3$  – vibrational temperature of the  $\nu_3$  vibration of CO<sub>2</sub>;
- $T_4$  – vibrational temperature of N<sub>2</sub>.

Vibrational temperatures are related to the average numbers of quanta  $e_x$  in the corresponding vibrations as follows:

$$\begin{aligned} e_2 &= \frac{2}{\exp(960/T_2) - 1} \\ e_3 &= \frac{1}{\exp(3380/T_3) - 1} \\ e_4 &= \frac{1}{\exp(3350/T_4) - 1} \end{aligned} \quad (4.7)$$

”2” in the first equation is due to 2-fold degeneracy of the energy levels of the bend vibration.

The dynamics of pumping/relaxation is described by the following equations

$$\begin{aligned}\frac{de_4}{dt} &= p_{e4} - r_a(e_4 - e_3) \\ \frac{de_3}{dt} &= p_{e3} + r_c(e_4 - e_3) - r_3 f_3 \\ \frac{de_2}{dt} &= f_2(p_{e2} + 3r_3 f_3 - r_2(e_2 - e_{2T}))\end{aligned}\tag{4.8}$$

where

$$\begin{aligned}p_{e4} &= 0.8 \times 10^{-3} \frac{q_4}{ny_2} W(t); \quad p_{e3} = 0.8 \times 10^{-3} \frac{q_3}{ny_1} W(t); \quad p_{e2} = 2.8 \times 10^{-3} \frac{q_2}{ny_1} W(t); \\ f_2 &= \frac{2(1+e_2)^2}{2+6e_2+3e_2^2}; \quad f_3 = e_3(1+e_2/2)^3 - (1+e_3)(e_2/2)^3 \exp(-500/T); \\ r_a &= kny_1; \quad r_c = kny_2; \quad r_2 = k_2 n; \quad r_3 = k_3 n; \\ k_2 &= \sum_{i=1}^3 y_i k_{2i}; \quad k_3 = \sum_{i=1}^3 y_i k_{3i}; \\ n &= 273 \frac{p[\text{bar}]}{T_0[\text{K}]}; \\ e_{2T} &= \frac{2}{\exp(960/T) - 1}\end{aligned}\tag{4.9}$$

where  $W(t)$  is the discharge power density measured in  $\text{kW}/\text{cm}^3$ ,  $p_e$  is measured in  $\mu\text{s}^{-1}$ , and the constants  $k$  are calculated using the following expressions [9, 10]:

$$\begin{aligned}k &= 240/T^{1/2}; \\ k_{31} &= A(t) \exp(4.138 + 7.945x - 631.24x^2 + 2239x^3); \\ k_{32} &= A(t) \exp(-1.863 + 213.3x - 2796.2x^2 + 9001.9x^3); \\ k_{33} &= A(t) \exp(-3.276 + 291.4x - 3831.8x^2 + 12688x^3); \\ k_{21} &= 1.16 \times 10^3 \exp(-59.3x); \\ k_{22} &= 8.55 \times 10^2 \exp(-69x); \\ k_{23} &= 1.3 \times 10^3 \exp(-40.6x)\end{aligned}\tag{4.10}$$

where  $x = T^{-1/3}$ ,  $A(t) = (T/273)(1 + e_{2T}/2)^{-3}$ , and temperature  $T$  is expressed in K.

Finally, the dynamics of the gas temperature is described by the following equation:

$$\frac{dT}{dt} = \frac{y_1}{C_V} (500r_3 f_3 + 960r_2(e_2 - e_{2T})) + 2.7 \frac{W(t)q_T}{nC_V},\tag{4.11}$$

where  $C_V = 2.5(y_1 + y_2) + 1.5y_3$ .

### 4.1.3 Optical pumping

In the case of optical pumping population dynamics is modelled with equations 4.7–4.11 with the exception of the expressions for excitation rates in Eq. 4.9 that are replaced by

$$\begin{aligned}p_{e4} &= 0; \\ p_{e3} &= \Phi\sigma; \\ p_{e2} &= \begin{cases} 0 & \text{direct excitation of } (00^01) \text{ at } \sim 4.3 \mu\text{m} \\ 2\Phi\sigma & \text{excitation via } (10^01, 02^01) \text{ at } \sim 2.8 \mu\text{m} \\ 4\Phi\sigma & \text{excitation via } (20^01, 12^01, 04^01) \text{ at } \sim 2.0 \mu\text{m} \end{cases}\end{aligned}\tag{4.12}$$

where  $\Phi$  is the flux of the pumping photons (number of photons per  $\text{m}^2$  per second), and  $\sigma$  is the absorption cross-section. Equations 4.12 imply that each pumping photon delivers one quantum of energy to the upper laser level, and zero, two or four quanta to the lower level, depending on the pumping transition.

## 4.2 Amplification

### 4.2.1 Laser transitions

Fig. 4.1 shows the vibrational levels and laser transitions included in the **co2amp** amplification model (because of the lack of the spectroscopic data, the sequence and hot bands currently are only supported for natural isotopologue of  $\text{CO}_2$  ( $626^1$ )).

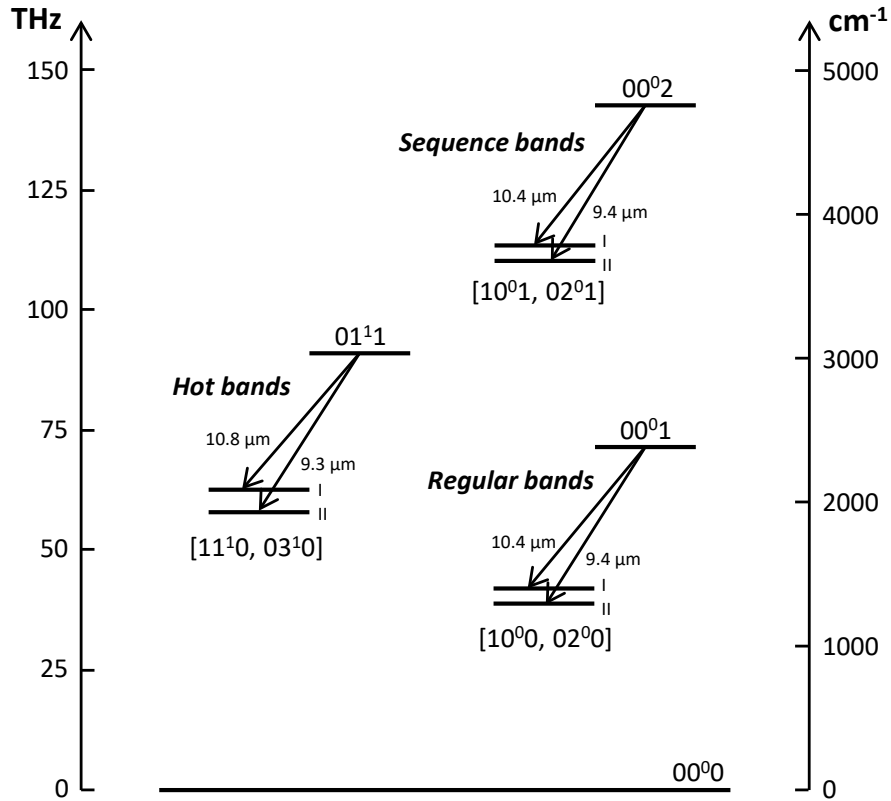


Figure 4.1: Vibrational transitions included in the amplification model. Wavelengths are given for natural  $\text{CO}_2$  isotopologue ( $626^1$ ).

### 4.2.2 Main equations

Amplification is simulated in the fast time-frame moving with the pulse using the following equations that also take into account rotational relaxation [11, 12]:

<sup>1</sup>A 3-digit notation commonly is used for designating the isotopologues (molecules with different isotopic composition) of carbon dioxide. In this notation 2, 3 and 4 correspondingly stand for  $^{12}\text{C}$ ,  $^{13}\text{C}$  and  $^{14}\text{C}$ ; 6, 7 and 8 represent correspondingly  $^{16}\text{O}$ ,  $^{17}\text{O}$  and  $^{18}\text{O}$ .  $626$  denotes a  $\text{CO}_2$  molecule with natural isotopic composition:  $^{16}\text{O}$ - $^{12}\text{C}$ - $^{16}\text{O}$ .

$$\begin{aligned}
\frac{\partial E}{\partial z} &= - \sum_J \rho_J, \\
\frac{\partial \rho_J}{\partial t} + \left( 2\pi i(\nu_c - \nu_{0J}) + \frac{1}{\tau_2} \right) \rho_J &= - \frac{\sigma_J n_J E}{2\tau_2}, \\
\frac{\partial n_J}{\partial t} + \frac{n_J - n_J^0}{\tau_R} &= 4(\rho_J E^* + c.c.),
\end{aligned} \tag{4.13}$$

where summation is done over all rotational-vibrational transitions of all CO<sub>2</sub> isotopologues, and

$E$  - complex field envelope,

$\rho_J$  - polarization of the medium,

$z$  - linear coordinate along the direction of beam propagation,

$t$  - time,

$n_J$  - population inversion of the transition (difference of population densities of upper and lower levels),

$n_J^0$  - equilibrium population inversion of the transition,

$\nu_c$  - carrier frequency,

$\nu_{0J}$  - transition frequency in the line center,

$\sigma_J$  - transition cross-section in the line center,

$\tau_2$  - polarization dephasing time,

$\tau_R$  - rotational relaxation time.

Transition frequencies of  $P$  and  $R$  transitions are calculated as follows:

$$\nu_J = \begin{cases} V + B_U(J-1)J - B_L J(J+1) & (P) \\ V + B_U(J+1)(J+2) - B_L J(J+1) & (R) \end{cases} \tag{4.14}$$

where  $J$  is the rotational quantum number,  $V$  is the vibrational constant of the corresponding transition, and,  $B_U$  and  $B_L$  the rotational constants of the upper and lower level of the transition correspondingly. The numerical values of the molecular constants used in the program are listed in Appendix B.

The transition cross-section in the line center is calculated [13]

$$\sigma_J [\text{m}^2] = \frac{(\lambda_J [\text{m}])^2 A_J [\text{s}^{-1}]}{4} \times \frac{\tau_2 [\text{s}]}{\pi} \tag{4.15}$$

where the first term defines the integral cross-section of the rotational line, and the second term is the maximum of the normalized Lorentzian profile of a line with width  $2\pi\Delta\nu_{HWHM} = 1/\tau_2$ .

Population inversion in the rotational equilibrium is calculated as

$$n_J^0 = \begin{cases} z(J-1)N_U - z(J)N_L & (P) \\ z(J+1)N_U - z(J)N_L & (R) \end{cases} \tag{4.16}$$

where  $N_U$  and  $N_L$  are the population densities of the corresponding upper and lower *vibrational* levels, and  $z(J)$  is the Boltzmann distribution:

$$z(J) = \begin{cases} 2 \frac{hB}{kT} (2J+1) \exp\left(-\frac{hB}{kT} J(J+1)\right) & (626, 636, 828, 838) \\ \frac{hB}{kT} (2J+1) \exp\left(-\frac{hB}{kT} J(J+1)\right) & (628, 638) \end{cases} \tag{4.17}$$

where  $h = 6.62606957 \times 10^{-34}$  J · s and  $k = 1.3806488 \times 10^{-23}$  J/K

Optical intensity  $I$  is related to the field amplitude as follows:

$$I [\text{W/m}^2] = 2h[J \cdot \text{s}] \nu_c [\text{s}^{-1}] |E|^2 \tag{4.18}$$



Dephasing and relaxation times are defined by the following equations:

$$\begin{aligned}\tau_2[\text{s}] &= \frac{10^{-6}}{\pi \times 7.61 \times 750 \times (P_{CO_2} + 0.733P_{N_2} + 0.64P_{He})} \\ \tau_R[\text{s}] &= \frac{10^{-7}}{750 \times (1.3P_{CO_2} + 1.2P_{N_2} + 0.6P_{He})}\end{aligned}\tag{4.19}$$

where pressure  $P$  is measured in bars.

## 4.2.3 Populations

In the approximation used in the **co2amp** model, the processes of pumping and vibrational relaxation are slow compared to the duration of the pulse. Thus, only the stimulated transitions contribute to the change of the populations of vibrational levels during the pulse.

In the fast time-frame associated with the pulse there is no equilibrium in the vibrational energy distribution, and a proper population dynamics rather than the temperature model must be used. Thus, during the amplification, population of each rotational-vibrational level is considered independently. After the pulse leaves the active medium, the energy distribution within each vibrational mode becomes normalized quickly, and can be described by the temperature model again.

An important simplification used in the model is the assumption that vibrational temperatures  $T_2$  and  $T_3$  are the same for all  $CO_2$  isotopologues. This assumption can be justified by the relatively small energy mismatch between vibrational levels of different isotopic species of the same molecule, and thus, fast inter-molecular V-V energy exchange. However, this assumption may not hold if the time-delay between two consecutive passes of a pulse through the amplifier is short compared to the relaxation times of intra-mode and inter-isotopic vibrational energy.

Initial populations of vibrational levels are calculated for each isotopologue and for each band using the following equations:

### Regular band

$$\begin{aligned}N_{00^0 1} &= \frac{N}{\mathcal{Q}} \exp\left(\frac{-3380}{T_3}\right) \\ N_{[10^0 0, 02^0 0]_{II}} &= N_{[10^0 0, 02^0 0]_{II}} = \frac{N}{\mathcal{Q}} \exp\left(\frac{-2 \times 960}{T_2}\right)\end{aligned}$$

### Sequence band

$$\begin{aligned}N_{00^0 2} &= \frac{N}{\mathcal{Q}} \exp\left(\frac{-2 \times 3380}{T_3}\right) \\ N_{[10^0 1, 02^0 1]_{II}} &= N_{[10^0 1, 02^0 1]_{II}} = \frac{N}{\mathcal{Q}} \exp\left(\frac{-2 \times 960}{T_2}\right) \exp\left(\frac{-3380}{T_3}\right)\end{aligned}\tag{4.20}$$

### Hot band

$$\begin{aligned}N_{01^1 1} &= \frac{N}{\mathcal{Q}} \exp\left(\frac{-3380}{T_3}\right) \exp\left(\frac{-960}{T_2}\right) \\ N_{[11^1 0, 03^1 0]_{II}} &= N_{[11^1 0, 03^1 0]_{II}} = \frac{N}{\mathcal{Q}} \exp\left(\frac{-3 \times 960}{T_2}\right)\end{aligned}$$

where  $N$  is the density of  $CO_2$  molecules, and  $\mathcal{Q}$  the partition function [14]:

$$\frac{1}{\mathcal{Q}} = \left(1 - \exp\left(\frac{-1920}{T_2}\right)\right) \times \left(1 - \exp\left(\frac{-3380}{T_3}\right)\right) \times \left(1 - \exp\left(\frac{-960}{T_2}\right)\right)^2\tag{4.21}$$

Change of the populations in the regular band due to stimulated transitions is calculated for each vibrational level using the last of the equations 4.13:

$$\begin{aligned}
\frac{d}{dt}N_{00^01} &= 2 \sum_{J(00^01 \rightarrow [10^00,02^00]_{II})} (\rho_J E^* + c.c.) \\
\frac{d}{dt}N_{[10^00,02^00]_I} &= -2 \sum_{J(00^01 \rightarrow [10^00,02^00]_I)} (\rho_J E^* + c.c.) \\
\frac{d}{dt}N_{[10^00,02^00]_{II}} &= -2 \sum_{J(00^01 \rightarrow [10^00,02^00]_{II})} (\rho_J E^* + c.c.)
\end{aligned} \tag{4.22}$$

where summation is done over all rotational transitions originating or ending at the corresponding vibrational level. Analogous equations are used for the sequence and the hot bands.

Changes of the average quantum numbers in the vibrational modes due to stimulated transitions are calculated as follows:

$$\begin{aligned}
\Delta e_3 &= \frac{\Delta N_U}{N}, \\
\Delta e_2 &= -2 \frac{\Delta N_U}{N} \times \frac{e'_2}{2e'_1 + e'_2}
\end{aligned} \tag{4.23}$$

wherein the last term in the second equation takes into account the equilibrium energy distribution between the coupled symmetric stretch and bending vibrations,  $e'_1 = \frac{1}{\exp\left(\frac{1920}{T_2}\right) - 1}$ ,  $e'_2 = \frac{2}{\exp\left(\frac{960}{T_2}\right) - 1}$ , and  $T_2$  is the vibrational temperature before the propagation of the pulse.

New vibrational temperatures are then calculated with Eq. 4.7.

# Appendices

# Appendix A

## Cross-sections of excitation processes

Effective cross-sections are expressed in Å; their numerical values in the nodes are given in the tables below (linear interpolation must be used for determining the values in intermediate points); the data and citations are reproduced from [4].

The following notation for cross-sections is used:

$Q_{m1}$  - Transport cross-section of CO<sub>2</sub> [15];

$Q_{m2}$  - Transport cross-section of N<sub>2</sub> [8];

$Q_{m3}$  - Transport cross-section of He [15];

$Q$  - Cross-section of resonant excitation of N<sub>2</sub> rotation [16, 17];

$Q_{11}$  - Cross-section of the process  $(000) \rightarrow (01^10)$  [15];

$Q_{12}$  - Cross-section of the process  $(000) \rightarrow (100 + 020)$  [15];

$Q_{13}...Q_{16}$  - Cross-sections of resonant processes around 3.8 eV [15];

$Q_{17}$  - Cross-section of the process  $(000) \rightarrow (001)$  [15];

$Q_{18}...Q_{1,10}$  - Cross-sections of electronic excitation and ionization of CO<sub>2</sub> [7];

$Q_{21}...Q_{28}$  - Cross-sections of the process  $N_2(v=0) \rightarrow N_2(v=1...8)$  [18, 19, 20];

$Q_{29}...Q_{2,15}$  - Cross-sections of electronic excitation and ionization of N<sub>2</sub> [20].

Table A.1: Cross-sections and energies for discharge pumping

$u_i$	$Q_{m1}$	$u_i$	$Q_{m2}$	$u_i$	$Q_{m3}$	$u_i$	$Q$
0	140	0	1.4	0	5	0.0015	0
0.04	84	0.001	1.4	0.01	5.4	0.05	0.1
0.1	55	0.002	1.6	0.1	5.8	0.25	0.65
0.3	21	0.008	2	0.2	6.2	0.5	1.15
0.5	10.8	0.01	2.2	1	6.5	0.8	2
0.6	9.4	0.04	4	2	6.1	1	2.65
1	5.7	0.08	6	7	5	1.5	5.6
1.7	5	0.1	6.5	10	4.1	1.8	7.5
2	5.1	0.2	8.8	20	3	1.9	8.2
2.5	6	0.3	9.8			2	8.6
3	7.7	0.4	10			2.15	8.95
4.1	9.4	1	10			2.43	9
5	14.5	1.2	11			2.6	8.9
7.4	10	1.4	12.5			2.75	8.4
10	11.7	1.8	20			2.9	7.65
20	16	2	25			3.25	6.2
27	16.3	2.5	30			3.6	5.1
50	13	3	26			4	4.5
		4	15			4.5	4.16
		5	12			5	3.97
		7	10			5.5	3.93
		10	10			7	4.17
		14	11			9	4.46
		18	12.2			11	4.42
		20	12			15	3.94
		30	10			22	3.15
		100	10			25	3.05

Table A.2: Cross-sections and energies for discharge pumping - continued

$u_i$	$Q_{11}$	$u_i$	$Q_{12}$	$u_i$	$Q_{13}$	$u_i$	$Q_{14}$	$u_i$	$Q_{15}$
0.083	0	0.167	0	0.252	0	2.37	0	2.37	0
0.085	0.36	0.2	0.54	2.7	0.25	3	0.26	3	0.17
0.09	1.04	0.25	0.82	3	0.4	3.5	0.52	3.65	0.33
0.1	1.6	0.3	0.82	3.3	0.6	4	0.5	3.8	0.31
0.12	1.84	0.5	0.68	3.6	0.65	4.5	0.22	4	0.21
0.14	2.12	0.7	0.56	4.5	0.23	4.6	0.1	4.3	0.1
0.16	2.16	1	0.47	4.6	0.1	5	0	5	0
0.2	2.08	1.4	0.45	5	0				
0.3	1.76	2	0.55						
0.4	1.52	3	1.15						
0.5	1.28	3.9	1.83						
0.6	1.08	4.5	1.4						
0.8	0.8	5	0.4						
1	0.58	6	0.28						
1.2	0.48	10	0.2						
1.6	0.34	20	0.1						
1.8	0.35								
2	0.4								
2.5	0.64								
3	1.04								
3.7	1.4								
4	1.36								
4.2	1.2								
4.5	0.92								
5	0.53								
6	0.4								
8	0.36								
9	0.28								
10	0.16								
10.1	0								
$u_{11} = 0.083 \text{ eV}$		$u_{12} = 0.167 \text{ eV}$		$u_{13} = 0.252 \text{ eV}$		$u_{14} = 0.339 \text{ eV}$		$u_{15} = 0.422 \text{ eV}$	
$u_i$	$Q_{16}$	$u_i$	$Q_{17}$	$u_i$	$Q_{18}$	$u_i$	$Q_{19}$	$u_i$	$Q_{1,10}$
2.5	0	0.29	0	7	0	10.5	0	13.8	0
3	0.19	0.3	0.44	8	0.5	11.5	0.56	15	0.1
3.6	0.245	0.35	0.65	8.4	0.6	14	0.8	16	0.13
4	0.21	0.4	0.73	9	0.46	20	1.2	17	0.17
5.07	0	0.5	0.84	10	0.175	30	2	30	1.55
		0.8	1	10.5	0	50	4	40	2.1
		1	1						
		2	0.78						
		6	0.37						
		10	0.25						
		50	0						
$u_{16} = 2.5 \text{ eV}$		$u_{17} = 0.29 \text{ eV}$		$u_{18} = 7 \text{ eV}$		$u_{19} = 10.5 \text{ eV}$		$u_{1,10} = 13.8 \text{ eV}$	

Table A.3: Cross-sections and energies for discharge pumping - continued

$u_i$	$Q_{21}$	$u_i$	$Q_{22}$	$u_i$	$Q_{23}$	$u_i$	$Q_{24}$	$u_i$	$Q_{25}$
0.29	0	1.83	0	1.9	0	2.05	0	2.1	0
0.5	0.0052	1.9	0.208	2	0.416	2.1	0.416	2.15	0.208
0.8	0.0083	2	1.46	2.1	1.33	2.2	1.16	2.2	0.541
1	0.0104	2.05	2.29	2.2	1.87	2.26	1.58	2.3	0.915
1.2	0.0166	2.1	1.66	2.3	1.25	2.55	0	2.46	1.12
1.3	0.0728	2.2	0.79	2.36	0.208	2.75	0.832	2.5	1.12
1.4	0.135	2.35	0.208	2.42	0	2.77	0	2.6	0.208
1.6	0.25	2.45	1.98	2.5	0.499	3	0.208	2.62	0
1.8	0.52	2.5	1.78	2.61	0.915	3.05	0.208	2.68	0
1.9	0.832	2.62	0.208	2.7	0.624	3.25	0	2.8	0.416
2	3.02	2.75	1.04	2.75	0.208			2.9	0.75
2.05	3.12	2.95	1.66	2.8	0			3	0
2.1	2.08	3.05	0.624	2.92	0.416			3.2	0.25
2.15	1.25	3.2	0.208	3	0.208			3.3	0.125
2.2	0.832	3.4	0.208	3.25	0.208			3.35	0
2.3	2.9	4	0	3.31	0				
2.45	1.04								
2.53	1.25								
2.6	1.75								
2.62	2.08								
2.68	1.73								
2.73	0.416								
2.85	0.32								
2.92	0.416								
3.12	0.728								
3.3	0.52								
4	0								
$u_{21} = 0.29$ eV		$u_{22} = 0.58$ eV		$u_{23} = 0.87$ eV		$u_{24} = 1.16$ eV		$u_{25} = 1.45$ eV	
$u_i$	$Q_{26}$	$u_i$	$Q_{27}$	$u_i$	$Q_{28}$	$u_i$	$Q_{29}$	$u_i$	$Q_{2,10}$
2.3	0	2.4	0	2.6	0	5	0	6.8	0
2.4	0.75	2.5	0.208	2.7	0.208	5.9	0.41	7.1	0.57
2.5	1.04	2.75	0.75	2.9	0.29	6.1	0.41	8.1	0.57
2.55	1.12	3	0	3	0.208	7	0.07	8.6	0.25
2.6	1.04	3.2	0.166	3.1	0	9	0	9.5	0.12
2.65	0.624	3.3	0.146	3.2	0			20.7	0
2.7	0.416	3.4	0	3.3	1.04				
2.8	0.208			3.4	0				
2.9	0.125								
3	2.5								
3.1	0.166								
3.2	0								
$u_{26} = 1.74$ eV		$u_{27} = 2.03$ eV		$u_{28} = 2.32$ eV		$u_{29} = 5$ eV		$u_{2,10} = 6.8$ eV	
$u_i$	$Q_{2,11}$	$u_i$	$Q_{2,12}$	$u_i$	$Q_{2,13}$	$u_i$	$Q_{2,14}$	$u_i$	$Q_{2,15}$
8.4	0	11.25	0	12.5	0	14	0	15.6	0
8.7	0.42	13.8	0.41	13	0.4	14.3	1.7	18	0.1
9.1	0.42	14	1	13.6	0.4	14.8	1.7	20	0.21
10	0.3	14.7	1	14	0.16	15.6	0.2	50	2.52
20.7	0	15	0.25	20.7	0	20.6	0.2	100	2.52
		65	0			25.4	2.8		
						100	2.8		
$u_{2,11} = 8.4$ eV		$u_{2,12} = 11.25$ eV		$u_{2,13} = 12.5$ eV		$u_{2,14} = 14$ eV		$u_{2,15} = 15.6$ eV	

## Appendix B

# Molecular constants

The vibrational and rotational constants  $V$  and  $B$  are listed in Table B.1.

Einstein coefficients  $A$  of the laser transitions included in the simulations are summarized in Tables B.2-B.7. Except for the sequence band of  $828$  isotopologue and the 10-micron transitions of  $838$  isotopologue, data are taken from the HITRAN2016 database [21] (Einstein coefficients) and our fit of HITRAN data with equation (4.14) ( $V$  and  $B$ ).

For the sequence band of  $828$  (not included in the HITRAN database),  $V$  constants are roughly estimated assuming same shift from  $628$  as in the regular band, and  $B$  constants are assumed to be  $\sim 1\%$  lower than that of regular and hot bands, in analogy with other isotopologues. Einstein coefficients are assumed  $\sim 2\times$  larger than those of the regular band in analogy with other isotopologues.

For the 10-micron transitions of  $838$  (not included in the HITRAN database),  $V$  and  $B$  constants are taken from [22]. Einstein coefficients are obtained by scaling the coefficients of the corresponding 9-micron transitions in the assumption that gain coefficients (proportional to transition cross-sections, Eq. 4.15) are roughly the same (according to Freed's measurements [23]).



Table B.1: Molecular constants of CO<sub>2</sub> isotopologues, THz

	626	628	828	636	638	838
00 <sup>0</sup> 1 → [10 <sup>0</sup> 0, 02 <sup>0</sup> 0] <sub>I,II</sub> ('Regular band')						
$V(00^0 1 - I)$	28.809	28.969	28.988	27.384	27.692	27.839
$V(00^0 1 - II)$	31.889	32.158	32.489	30.508	30.610	30.786
$B(00^0 1)$	0.011589	0.010936	0.010303	0.011593	0.010939	0.010315
$B([10^0 0, 02^0 0]_I)$	0.011683	0.011034	0.010403	0.011668	0.011019	0.010403
$B([10^0 0, 02^0 0]_{II})$	0.011687	0.011019	0.010375	0.011700	0.011031	0.010394
00 <sup>0</sup> 2 → [10 <sup>0</sup> 1, 02 <sup>0</sup> 1] <sub>I,II</sub> ('Sequence band')						
$V(00^0 2 - I)$	28.737	28.911	[28.93]	27.300	-	-
$V(00^0 2 - II)$	31.792	32.029	[32.36]	30.453	-	-
$B(00^0 2)$	0.011497	0.010859	[0.0103]	0.011512	-	-
$B([10^0 1, 02^0 1]_I)$	0.011588	0.010955	[0.0103]	0.011585	-	-
$B([10^0 1, 02^0 1]_{II})$	0.011598	0.010946	[0.0103]	0.011623	-	-
01 <sup>1e</sup> 1 → [11 <sup>1e</sup> 0, 03 <sup>1e</sup> 0] <sub>I,II</sub> ('Hot-e band')						
$V(01^{1e} 1 - I)$	27.796	27.964	20.190	26.476	26.749	-
$V(01^{1e} 1 - II)$	32.124	32.388	32.690	30.689	30.832	-
$B(01^{1e} 1)$	0.011602	0.010949	0.010324	0.011605	0.010953	-
$B([11^{1e} 0, 03^{1e} 0]_I)$	0.011687	0.011036	0.010412	0.011676	0.011028	-
$B([11^{1e} 0, 03^{1e} 0]_{II})$	0.011695	0.011032	0.010398	0.011702	0.011040	-
01 <sup>1f</sup> 1 → [11 <sup>1f</sup> 0, 03 <sup>1f</sup> 0] <sub>I,II</sub> ('Hot-f band')						
$V(01^{1f} 1 - I)$	27.796	27.964	28.019	26.476	26.749	-
$V(01^{1f} 1 - II)$	32.124	32.388	32.690	30.689	30.832	-
$B(01^{1f} 1)$	0.011620	0.010965	0.010338	0.011623	0.010970	-
$B([11^{1f} 0, 03^{1f} 0]_I)$	0.011716	0.011063	0.010437	0.011703	0.011053	-
$B([11^{1f} 0, 03^{1f} 0]_{II})$	0.011723	0.011055	0.010417	0.011733	0.011066	-

Table B.2: Einstein coefficients  $A$  of laser transitions of  $'626'$  CO<sub>2</sub>, s<sup>-1</sup>

$J$	Regular			Sequence			Hot-e			Hot-f		
	10P	10R	9P	9R	10P	10R	9P	9R	10P	10R	9P	9R
0	-	0.130	-	0.145	-	-	-	-	-	-	-	-
1	-	-	-	-	0.809	0.324	0.800	0.322	-	-	-	-
2	0.260	0.168	0.289	0.187	-	-	-	-	0.176	0.135	0.216	0.166
3	-	-	-	-	0.484	0.361	0.478	0.359	-	-	-	-
4	0.222	0.178	0.247	0.199	-	-	-	-	0.188	0.155	0.231	0.191
5	-	-	-	-	0.447	0.376	0.442	0.374	-	-	-	-
6	0.212	0.184	0.235	0.205	-	-	-	-	0.186	0.162	0.227	0.201
7	-	-	-	-	0.432	0.384	0.427	0.383	-	-	-	-
8	0.206	0.186	0.229	0.209	-	-	-	-	0.184	0.166	0.225	0.206
9	-	-	-	-	0.423	0.389	0.418	0.389	-	-	-	-
10	0.203	0.188	0.225	0.212	-	-	-	-	0.182	0.169	0.222	0.210
11	-	-	-	-	0.417	0.392	0.413	0.394	-	-	-	-
12	0.200	0.190	0.223	0.215	-	-	-	-	0.180	0.170	0.220	0.212
13	-	-	-	-	0.412	0.395	0.409	0.398	-	-	-	-
14	0.198	0.191	0.221	0.217	-	-	-	-	0.179	0.172	0.219	0.215
15	-	-	-	-	0.408	0.396	0.406	0.401	-	-	-	-
16	0.196	0.192	0.219	0.218	-	-	-	-	0.177	0.172	0.217	0.217
17	-	-	-	-	0.405	0.398	0.403	0.405	-	-	-	-
18	0.195	0.192	0.218	0.220	-	-	-	-	0.176	0.173	0.216	0.218
19	-	-	-	-	0.402	0.399	0.401	0.408	-	-	-	-
20	0.193	0.192	0.217	0.222	-	-	-	-	0.175	0.173	0.215	0.220
21	-	-	-	-	0.399	0.399	0.400	0.411	-	-	-	-
22	0.192	0.193	0.216	0.223	-	-	-	-	0.174	0.174	0.214	0.222
23	-	-	-	-	0.396	0.400	0.398	0.414	-	-	-	-
24	0.190	0.193	0.215	0.225	-	-	-	-	0.173	0.172	0.213	0.223
25	-	-	-	-	0.393	0.400	0.397	0.417	-	-	-	-
26	0.189	0.193	0.215	0.226	-	-	-	-	0.175	0.172	0.212	0.224
27	-	-	-	-	0.390	0.400	0.396	0.420	-	-	-	-
28	0.188	0.193	0.214	0.228	-	-	-	-	0.174	0.172	0.211	0.226
29	-	-	-	-	0.387	0.400	0.395	0.423	-	-	-	-
30	0.186	0.192	0.214	0.229	-	-	-	-	0.173	0.172	0.210	0.227
31	-	-	-	-	0.384	0.399	0.394	0.425	-	-	-	-
32	0.185	0.192	0.213	0.231	-	-	-	-	0.172	0.172	0.209	0.229
33	-	-	-	-	0.381	0.399	0.393	0.428	-	-	-	-
34	0.183	0.192	0.213	0.232	-	-	-	-	0.171	0.171	0.208	0.230
35	-	-	-	-	0.378	0.398	0.393	0.432	-	-	-	-
36	0.182	0.191	0.212	0.234	-	-	-	-	0.169	0.173	0.211	0.230
37	-	-	-	-	0.375	0.397	0.392	0.435	-	-	-	-
38	0.181	0.191	0.212	0.236	-	-	-	-	0.166	0.173	0.210	0.233
39	-	-	-	-	0.372	0.396	0.392	0.438	-	-	-	-
40	0.179	0.190	0.212	0.237	-	-	-	-	0.164	0.173	0.210	0.234
41	-	-	-	-	0.369	0.395	0.392	0.441	-	-	-	-
42	0.177	0.190	0.212	0.239	-	-	-	-	0.163	0.172	0.209	0.236
43	-	-	-	-	0.366	0.393	0.391	0.444	-	-	-	-
44	0.176	0.189	0.211	0.241	-	-	-	-	0.161	0.171	0.209	0.237
45	-	-	-	-	0.363	0.392	0.391	0.447	-	-	-	-
46	0.174	0.188	0.211	0.242	-	-	-	-	0.159	0.171	0.208	0.239
47	-	-	-	-	0.359	0.390	0.391	0.451	-	-	-	-
48	0.173	0.187	0.211	0.244	-	-	-	-	0.158	0.170	0.208	0.240
49	-	-	-	-	0.356	0.388	0.391	0.454	-	-	-	-
50	0.171	0.186	0.211	0.246	-	-	-	-	0.157	0.169	0.208	0.242
51	-	-	-	-	0.352	0.387	0.391	0.458	-	-	-	-
52	0.169	0.185	0.211	0.248	-	-	-	-	0.155	0.168	0.207	0.243
53	-	-	-	-	0.349	0.385	0.391	0.461	-	-	-	-
54	0.167	0.184	0.211	0.249	-	-	-	-	0.154	0.167	0.207	0.245
55	-	-	-	-	0.345	0.382	0.391	0.465	-	-	-	-
56	0.166	0.183	0.211	0.251	-	-	-	-	0.153	0.167	0.207	0.246
57	-	-	-	-	0.342	0.380	0.391	0.468	-	-	-	-
58	0.164	0.182	0.211	0.253	-	-	-	-	0.151	0.166	0.207	0.248
59	-	-	-	-	0.338	0.377	0.392	0.472	-	-	-	-
60	0.162	-	0.211	-	-	-	-	-	0.150	-	0.207	-

Table B.3: Einstein coefficients  $A$  of laser transitions of  ${}^{628}\text{CO}_2$ ,  $\text{s}^{-1}$ 

$J$	Regular			Sequence			Hot-e			Hot-f		
	10P	10R	9P	10P	10R	9P	10P	10R	9P	10P	10R	9P
0	-	0.100	-	-	-	-	-	-	-	-	-	-
1	0.298	0.120	0.574	-	-	-	0.162	0.089	-	0.162	0.089	-
2	0.199	0.128	0.382	-	-	-	0.206	0.148	0.268	0.206	0.148	0.268
3	0.179	0.133	0.343	-	-	0.642	0.481	0.158	0.285	0.157	0.124	0.285
4	0.170	0.136	0.326	-	0.287	0.611	0.493	0.158	0.286	0.158	0.130	0.286
5	0.165	0.139	0.317	0.348	0.292	0.593	0.501	0.157	0.284	0.157	0.133	0.284
6	0.162	0.140	0.311	0.341	0.295	0.581	0.508	0.156	0.282	0.156	0.136	0.282
7	0.159	0.141	0.306	0.336	0.298	0.573	0.513	0.155	0.280	0.155	0.138	0.280
8	0.158	0.142	0.303	0.332	0.300	0.567	0.517	0.154	0.278	0.154	0.139	0.278
9	0.156	0.143	0.300	0.329	0.302	0.562	0.521	0.154	0.277	0.153	0.140	0.277
10	0.155	0.144	0.298	0.327	0.303	0.558	0.524	0.153	0.275	0.152	0.141	0.276
11	0.154	0.144	0.296	0.324	0.304	0.555	0.527	0.152	0.274	0.151	0.142	0.275
12	0.153	0.145	0.295	0.323	0.305	0.552	0.530	0.152	0.273	0.151	0.143	0.273
13	0.152	0.145	0.294	0.321	0.306	0.549	0.532	0.151	0.272	0.150	0.143	0.273
14	0.152	0.145	0.292	0.319	0.307	0.547	0.534	0.151	0.271	0.150	0.144	0.272
15	0.151	0.146	0.291	0.318	0.307	0.545	0.537	0.150	0.270	0.149	0.144	0.271
16	0.150	0.146	0.290	0.316	0.308	0.543	0.538	0.150	0.269	0.149	0.144	0.270
17	0.150	0.146	0.289	0.315	0.308	0.542	0.541	0.149	0.268	0.148	0.144	0.269
18	0.149	0.146	0.289	0.314	0.309	0.540	0.542	0.149	0.268	0.148	0.145	0.269
19	0.148	0.146	0.288	0.312	0.309	0.539	0.544	0.148	0.267	0.147	0.145	0.268
20	0.148	0.146	0.287	0.311	0.309	0.538	0.546	0.148	0.266	0.147	0.145	0.267
21	0.147	0.147	0.287	0.310	0.309	0.537	0.548	0.148	0.266	0.146	0.145	0.267
22	0.147	0.147	0.286	0.309	0.309	0.535	0.550	0.147	0.265	0.146	0.145	0.266
23	0.146	0.147	0.285	0.308	0.309	0.534	0.551	0.147	0.264	0.145	0.145	0.266
24	0.146	0.147	0.285	0.307	0.309	0.533	0.553	0.147	0.264	0.145	0.145	0.265
25	0.145	0.146	0.284	0.305	0.309	0.532	0.555	0.146	0.263	0.144	0.145	0.265
26	0.144	0.146	0.284	0.304	0.309	0.532	0.556	0.146	0.262	0.144	0.145	0.264
27	0.144	0.146	0.283	0.303	0.309	0.531	0.558	0.145	0.262	0.143	0.145	0.264
28	0.143	0.146	0.283	0.302	0.309	0.530	0.559	0.145	0.262	0.143	0.145	0.263
29	0.143	0.146	0.282	0.301	0.309	0.529	0.561	0.145	0.261	0.142	0.145	0.263
30	0.142	0.146	0.282	0.300	0.308	0.528	0.563	0.144	0.261	0.142	0.145	0.263
31	0.142	0.146	0.282	0.301	0.308	0.528	0.564	0.144	0.260	0.141	0.145	0.262
32	0.141	0.146	0.281	0.297	0.308	0.527	0.566	0.144	0.260	0.141	0.145	0.262
33	0.141	0.146	0.281	-	-	0.526	0.568	0.143	0.259	0.141	0.145	0.261
34	0.140	0.145	0.280	-	-	0.526	0.569	0.143	0.259	0.140	0.145	0.261
35	0.139	0.145	0.280	-	-	0.525	0.570	0.142	0.259	0.139	0.144	0.261
36	0.139	0.145	0.280	-	-	0.525	0.572	0.142	0.258	0.139	0.144	0.260
37	0.138	0.145	0.279	-	-	0.524	0.574	0.142	0.258	0.138	0.144	0.260
38	0.138	0.144	0.279	-	-	0.523	0.575	0.141	0.257	0.138	0.144	0.260
39	0.137	0.144	0.279	-	-	0.523	0.577	0.141	0.257	0.137	0.144	0.259
40	0.136	0.144	0.279	-	-	0.522	0.579	0.140	0.256	0.137	0.144	0.259
41	0.136	0.143	0.278	-	-	-	-	0.140	0.256	0.136	0.143	0.259
42	0.135	0.143	0.278	-	-	-	-	0.139	0.256	0.136	0.143	0.258
43	0.134	0.143	0.278	-	-	-	-	0.139	0.255	0.135	0.143	0.258
44	0.134	0.142	0.277	-	-	-	-	0.139	0.255	0.135	0.143	0.258
45	0.133	0.142	0.277	-	-	-	-	0.138	0.255	0.134	0.142	0.258
46	0.133	0.142	0.277	-	-	-	-	0.138	0.254	0.133	0.142	0.257
47	0.132	0.141	0.277	-	-	-	-	0.137	0.254	0.133	0.142	0.257
48	0.131	0.141	0.277	-	-	-	-	0.137	0.254	0.132	0.141	0.257
49	0.131	0.140	0.276	-	-	-	-	0.136	0.253	0.132	0.141	0.257
50	0.130	0.140	0.276	-	-	-	-	0.136	0.253	0.131	0.141	0.256
51	0.129	0.140	0.276	-	-	-	-	0.135	0.253	0.131	0.140	0.256
52	0.128	0.139	0.276	-	-	-	-	0.135	0.252	0.130	0.140	0.256
53	0.128	0.139	0.276	-	-	-	-	0.134	0.252	0.129	0.140	0.256
54	0.127	0.138	0.276	-	-	-	-	0.134	0.252	0.129	0.139	0.256
55	0.126	0.138	0.275	-	-	-	-	0.133	0.251	0.128	0.139	0.255
56	0.126	0.137	0.275	-	-	-	-	0.133	0.251	0.128	0.138	0.255
57	0.125	0.137	0.275	-	-	-	-	0.132	0.251	0.127	0.138	0.255
58	0.124	0.136	0.275	-	-	-	-	0.132	0.251	0.126	0.137	0.255
59	0.123	0.135	0.275	-	-	-	-	0.131	0.250	0.126	0.137	0.255
60	0.123	-	0.275	-	-	-	-	0.131	0.250	0.125	-	0.254

Table B.4: Einstein coefficients  $A$  of laser transitions of  $^{828}\text{CO}_2$ ,  $\text{s}^{-1}$ 

$J$	Regular			Sequence			Hot-e			Hot-f		
	10P	10R	9R	10P	10R	9P	10P	10R	9P	10P	10R	9R
0	-	0.073	-	0.234	-	-	-	-	-	-	-	-
1	-	-	-	-	[0.2]	[0.7]	-	-	-	-	-	-
2	0.146	0.094	0.466	0.301	-	-	-	-	-	-	0.318	0.243
3	-	-	-	-	[0.2]	[0.7]	-	-	0.337	-	-	-
4	0.125	0.100	0.398	0.321	-	-	-	-	-	-	0.105	0.338
5	-	-	-	-	[0.2]	[0.7]	-	-	-	-	-	0.280
6	0.119	0.103	0.379	0.330	-	-	0.128	0.108	0.336	0.127	0.111	0.334
7	-	-	-	-	[0.2]	[0.7]	0.127	0.112	0.332	-	-	-
8	0.116	0.104	0.368	0.337	-	-	0.125	0.114	0.328	0.125	0.113	0.330
9	-	-	-	-	[0.2]	[0.7]	-	-	-	-	-	-
10	0.114	0.105	0.363	0.340	-	-	0.124	0.115	0.325	0.124	0.115	0.327
11	-	-	-	-	[0.2]	[0.7]	0.123	0.116	0.322	0.123	0.116	0.324
12	0.112	0.106	0.360	0.343	-	-	0.122	0.116	0.320	-	-	0.310
13	-	-	-	-	[0.2]	[0.7]	-	-	-	0.122	0.117	0.322
14	0.111	0.106	0.356	0.347	-	-	0.122	0.117	0.318	-	-	0.313
15	-	-	-	-	[0.2]	[0.7]	-	-	-	0.121	0.117	0.320
16	0.110	0.107	0.353	0.349	-	-	0.121	0.117	0.317	-	-	0.317
17	-	-	-	-	[0.2]	[0.7]	-	-	-	0.120	0.118	0.318
18	0.109	0.107	0.351	0.351	-	-	0.120	0.117	0.315	-	-	-
19	-	-	-	-	[0.2]	[0.7]	-	-	-	0.119	0.118	0.317
20	0.108	0.107	0.349	0.353	-	-	0.120	0.117	0.315	-	-	0.320
21	-	-	-	-	[0.2]	[0.7]	-	-	-	0.119	0.118	0.315
22	0.108	0.107	0.348	0.355	-	-	0.120	0.117	0.314	0.119	0.118	0.322
23	-	-	-	-	[0.2]	[0.7]	-	-	-	0.118	0.118	0.324
24	0.107	0.107	0.346	0.357	-	-	0.119	0.117	0.312	-	-	-
25	-	-	-	-	[0.2]	[0.7]	-	-	-	0.117	0.118	0.325
26	0.106	0.107	0.346	0.359	-	-	0.119	0.117	0.311	-	-	0.327
27	-	-	-	-	[0.2]	[0.7]	-	-	-	0.116	0.118	0.312
28	0.105	0.107	0.343	0.360	-	-	0.118	0.117	0.310	-	-	-
29	-	-	-	-	[0.2]	[0.7]	0.117	0.117	0.309	0.116	0.118	0.328
30	0.105	0.107	0.342	0.362	-	-	0.117	0.116	0.307	-	-	-
31	-	-	-	-	[0.2]	[0.7]	-	-	-	0.115	0.118	0.330
32	0.104	0.106	0.341	0.364	-	-	-	-	0.307	-	0.309	0.332
33	-	-	-	-	[0.2]	[0.7]	-	-	-	-	-	0.333
34	0.103	0.106	0.340	0.365	-	-	-	-	0.305	-	0.308	-
35	-	-	-	-	[0.2]	[0.7]	-	-	-	-	-	0.334
36	0.102	0.106	0.340	0.367	-	-	-	-	0.305	-	0.307	0.336
37	-	-	-	-	[0.2]	[0.7]	-	-	-	-	-	-
38	0.101	0.105	0.339	0.369	-	-	-	-	0.304	-	0.306	0.337
39	-	-	-	-	[0.2]	[0.7]	-	-	-	-	-	-
40	0.100	0.104	0.338	0.370	-	-	-	-	0.302	-	0.305	0.338
41	-	-	-	-	[0.2]	[0.7]	-	-	-	-	-	0.342
42	0.100	0.104	0.337	0.372	-	-	-	-	-	-	-	-
43	-	-	-	-	[0.2]	[0.7]	-	-	-	-	-	-
44	0.098	0.104	0.336	0.373	-	-	-	-	-	-	-	-
45	-	-	-	-	[0.2]	[0.7]	-	-	-	-	-	-
46	0.097	0.103	0.335	0.375	-	-	-	-	0.301	-	0.304	0.342
47	-	-	-	-	[0.2]	[0.7]	-	-	-	-	-	-
48	0.096	0.103	0.335	0.376	-	-	-	-	0.300	-	-	-
49	-	-	-	-	[0.2]	[0.7]	-	-	-	-	-	-
50	0.095	0.102	0.333	0.378	-	-	-	-	-	-	-	-
51	-	-	-	-	[0.2]	[0.7]	-	-	-	-	-	-
52	0.095	0.101	0.333	0.378	-	-	-	-	-	-	-	-
53	-	-	-	-	[0.2]	[0.7]	-	-	-	-	-	-
54	0.093	0.100	0.332	0.381	-	-	-	-	-	-	-	-
55	-	-	-	-	[0.2]	[0.7]	-	-	-	-	-	-
56	0.092	0.099	0.331	0.382	-	-	-	-	-	-	-	-
57	-	-	-	-	[0.2]	[0.7]	-	-	-	-	-	-
58	-	-	0.331	0.384	-	-	-	-	-	-	-	-
59	-	-	-	-	[0.2]	[0.7]	-	-	-	-	-	-
60	-	-	0.331	-	-	-	-	-	-	-	-	-

Table B.5: Einstein coefficients  $A$  of laser transitions of  $^{13}\text{C}^{18}\text{O}_2$ ,  $\text{s}^{-1}$ 

$J$	Regular			Sequence			Hot-e			Hot-f		
	10P	10R	9P	9R	10P	10R	9P	9R	10P	10R	9P	9R
0	-	0.138	-	0.072	-	-	-	-	-	-	-	-
1	-	-	-	-	0.833	0.335	-	0.158	-	-	-	-
2	0.276	0.178	0.143	0.093	-	-	-	0.075	0.175	0.134	0.124	0.095
3	-	-	-	-	0.500	0.374	0.235	0.176	-	0.134	-	-
4	0.237	0.190	0.122	0.099	-	-	-	-	0.188	0.154	0.132	0.109
5	-	-	-	-	0.462	0.389	0.217	0.184	0.187	-	-	-
6	0.225	0.195	0.116	0.102	-	-	-	-	0.185	0.162	0.130	0.115
7	-	-	-	-	0.447	0.397	0.209	0.188	0.185	0.164	0.129	0.117
8	0.219	0.198	0.113	0.104	-	-	-	-	0.183	0.166	0.129	0.118
9	-	-	-	-	0.438	0.403	0.205	0.191	0.183	0.167	0.128	0.120
10	0.215	0.200	0.111	0.105	-	-	-	-	0.181	0.168	0.127	0.121
11	-	-	-	-	0.431	0.406	0.202	0.194	0.179	0.171	0.126	0.122
12	0.213	0.202	0.110	0.107	-	-	-	-	0.179	0.171	0.125	0.123
13	-	-	-	-	0.428	0.409	0.200	0.196	0.176	0.173	0.125	0.124
14	0.210	0.203	0.109	0.108	-	-	-	-	0.176	0.173	0.125	0.124
15	-	-	-	-	0.422	0.413	0.199	0.198	0.176	0.173	0.124	0.126
16	0.209	0.204	0.108	0.109	-	-	-	-	0.174	0.174	0.124	0.127
17	-	-	-	-	0.419	0.414	0.198	0.200	0.174	0.174	0.123	0.127
18	0.207	0.204	0.108	0.110	-	-	-	-	0.174	0.174	0.122	0.129
19	-	-	-	-	0.415	0.415	0.197	0.201	0.172	0.174	0.122	0.129
20	0.206	0.205	0.107	0.111	-	-	-	-	0.172	0.174	0.122	0.129
21	-	-	-	-	0.414	0.416	0.196	0.203	0.172	0.174	0.122	0.129
22	0.205	0.206	0.107	0.112	-	-	-	-	0.172	0.174	0.122	0.129
23	-	-	-	-	0.411	0.416	0.195	0.205	0.172	0.174	0.122	0.129
24	0.203	0.206	0.106	0.112	-	-	-	-	0.172	0.174	0.122	0.129
25	-	-	-	-	0.409	0.417	0.195	0.206	0.172	0.174	0.122	0.129
26	0.202	0.207	0.106	0.113	-	-	-	-	0.172	0.174	0.122	0.129
27	-	-	-	-	0.406	0.418	0.194	0.208	0.172	0.174	0.122	0.129
28	0.201	0.207	0.106	0.114	-	-	-	-	0.172	0.174	0.122	0.129
29	-	-	-	-	0.403	0.418	0.194	0.210	0.172	0.174	0.122	0.129
30	0.199	0.207	0.105	0.114	-	-	-	-	0.172	0.174	0.122	0.129
31	-	-	-	-	0.401	0.419	0.193	0.212	0.172	0.174	0.122	0.129
32	0.197	0.207	0.105	0.116	-	-	-	-	0.172	0.174	0.122	0.129
33	-	-	-	-	0.398	0.419	0.193	0.214	0.172	0.174	0.122	0.129
34	0.197	0.206	0.105	0.117	-	-	-	-	0.172	0.174	0.122	0.129
35	-	-	-	-	0.396	0.418	0.193	0.215	0.172	0.174	0.122	0.129
36	0.196	0.207	0.105	0.118	-	-	-	-	0.172	0.174	0.122	0.129
37	-	-	-	-	0.394	0.418	0.193	0.217	0.172	0.174	0.122	0.129
38	0.194	0.206	0.105	0.119	-	-	-	-	0.172	0.174	0.122	0.129
39	-	-	-	-	0.390	0.419	0.193	0.219	0.172	0.174	0.122	0.129
40	0.193	0.206	0.105	0.120	-	-	-	-	0.172	0.174	0.122	0.129
41	-	-	-	-	0.389	0.417	0.192	0.220	0.172	0.174	0.122	0.129
42	0.192	0.206	0.105	0.121	-	-	-	-	0.172	0.174	0.122	0.129
43	-	-	-	-	0.385	0.418	-	-	0.172	0.174	0.122	0.129
44	0.190	0.206	0.105	0.122	-	-	-	-	0.172	0.174	0.122	0.129
45	-	-	-	-	-	-	-	-	0.172	0.174	0.122	0.129
46	0.189	0.205	0.105	0.123	-	-	-	-	0.172	0.174	0.122	0.129
47	-	-	-	-	-	-	-	-	0.172	0.174	0.122	0.129
48	0.187	0.204	0.105	0.123	-	-	-	-	0.172	0.174	0.122	0.129
49	-	-	-	-	-	-	-	-	0.172	0.174	0.122	0.129
50	0.186	0.203	0.105	0.125	-	-	-	-	0.172	0.174	0.122	0.129
51	-	-	-	-	-	-	-	-	0.172	0.174	0.122	0.129
52	0.185	0.203	0.105	0.126	-	-	-	-	0.172	0.174	0.122	0.129
53	-	-	-	-	-	-	-	-	0.172	0.174	0.122	0.129
54	0.183	0.203	0.105	0.127	-	-	-	-	0.172	0.174	0.122	0.129
55	-	-	-	-	-	-	-	-	0.172	0.174	0.122	0.129
56	0.182	0.202	0.105	0.128	-	-	-	-	0.172	0.174	0.122	0.129
57	-	-	-	-	-	-	-	-	0.172	0.174	0.122	0.129
58	0.180	0.201	0.105	0.129	-	-	-	-	0.172	0.174	0.122	0.129
59	-	-	-	-	-	-	-	-	0.172	0.174	0.122	0.129
60	0.178	-	0.105	-	-	-	-	-	0.172	0.174	0.122	0.129

Table B.6: Einstein coefficients  $A$  of laser transitions of  $'638'$  CO<sub>2</sub>, s<sup>-1</sup>

$J$	Regular			Sequence			Hot-e			Hot-f		
	10P	10R	9P	10P	10R	9P	10P	10R	9P	10P	10R	9P
0	-	0.117	-	-	-	-	-	0.093	-	-	0.093	-
1	0.350	0.141	0.315	0.106	-	-	-	0.098	-	-	0.098	-
2	0.233	0.151	0.210	0.127	-	-	-	0.118	0.125	0.155	0.118	0.163
3	0.210	0.157	0.189	0.136	-	-	-	0.165	0.137	0.165	0.130	0.173
4	0.199	0.160	0.179	0.145	-	-	-	0.166	0.174	0.165	0.136	0.174
5	0.194	0.163	0.174	0.147	-	-	-	0.165	0.139	0.164	0.140	0.173
6	0.190	0.165	0.171	0.149	-	-	-	0.164	0.142	0.163	0.142	0.171
7	0.187	0.166	0.168	0.151	-	-	-	0.163	0.144	0.162	0.144	0.170
8	0.185	0.167	0.166	0.152	-	-	-	0.162	0.145	0.161	0.146	0.169
9	0.183	0.168	0.165	0.153	-	-	-	0.161	0.147	0.160	0.147	0.168
10	0.182	0.169	0.164	0.154	-	-	-	0.160	0.147	0.159	0.148	0.167
11	0.181	0.170	0.163	0.155	-	-	-	0.159	0.148	0.159	0.149	0.167
12	0.180	0.170	0.162	0.156	-	-	-	0.158	0.149	0.158	0.150	0.166
13	0.179	0.171	0.161	0.157	-	-	-	0.157	0.150	0.157	0.150	0.165
14	0.178	0.171	0.161	0.158	-	-	-	0.156	0.151	0.156	0.151	0.164
15	0.177	0.172	0.160	0.158	-	-	-	0.155	0.152	0.155	0.152	0.163
16	0.176	0.172	0.160	0.159	-	-	-	0.154	0.153	0.154	0.153	0.162
17	0.176	0.172	0.159	0.160	-	-	-	0.153	0.154	0.153	0.154	0.161
18	0.175	0.173	0.159	0.160	-	-	-	0.152	0.155	0.152	0.155	0.163
19	0.174	0.173	0.158	0.161	-	-	-	0.151	0.156	0.151	0.156	0.163
20	0.174	0.173	0.158	0.161	-	-	-	0.150	0.157	0.150	0.157	0.162
21	0.173	0.173	0.158	0.162	-	-	-	0.149	0.158	0.149	0.158	0.162
22	0.173	0.173	0.157	0.162	-	-	-	0.148	0.159	0.148	0.159	0.161
23	0.172	0.173	0.157	0.163	-	-	-	0.147	0.160	0.147	0.160	0.161
24	0.171	0.173	0.157	0.164	-	-	-	0.146	0.161	0.146	0.161	0.162
25	0.171	0.173	0.157	0.164	-	-	-	0.145	0.162	0.145	0.162	0.163
26	0.170	0.173	0.156	0.165	-	-	-	0.144	0.163	0.144	0.163	0.164
27	0.170	0.173	0.156	0.165	-	-	-	0.143	0.164	0.143	0.164	0.165
28	0.169	0.173	0.156	0.166	-	-	-	0.142	0.165	0.142	0.165	0.166
29	0.168	0.173	0.156	0.166	-	-	-	0.141	0.166	0.141	0.166	0.167
30	0.168	0.173	0.156	0.167	-	-	-	0.140	0.167	0.140	0.167	0.168
31	0.167	0.173	0.155	0.168	-	-	-	0.139	0.168	0.139	0.168	0.169
32	0.167	0.173	0.155	0.168	-	-	-	0.138	0.169	0.138	0.169	0.170
33	0.166	0.173	0.155	0.169	-	-	-	0.137	0.170	0.137	0.170	0.171
34	0.166	0.173	0.155	0.169	-	-	-	0.136	0.171	0.136	0.171	0.172
35	0.165	0.173	0.155	0.170	-	-	-	0.135	0.172	0.135	0.172	0.173
36	0.164	0.173	0.155	0.171	-	-	-	0.134	0.173	0.134	0.173	0.174
37	0.164	0.173	0.155	0.171	-	-	-	0.133	0.174	0.133	0.174	0.175
38	0.163	0.172	0.155	0.172	-	-	-	0.132	0.175	0.132	0.175	0.176
39	0.162	0.172	0.155	0.172	-	-	-	0.131	0.176	0.131	0.176	0.177
40	0.162	0.172	0.154	0.173	-	-	-	0.130	0.177	0.130	0.177	0.178
41	0.161	0.172	0.154	0.174	-	-	-	0.129	0.178	0.129	0.178	0.179
42	0.161	0.172	0.154	0.174	-	-	-	0.128	0.179	0.128	0.179	0.180
43	0.160	0.171	0.154	0.175	-	-	-	0.127	0.180	0.127	0.180	0.181
44	0.159	0.171	0.154	0.175	-	-	-	0.126	0.181	0.126	0.181	0.182
45	0.159	0.171	0.154	0.176	-	-	-	0.125	0.182	0.125	0.182	0.183
46	0.158	0.170	0.154	0.177	-	-	-	0.124	0.183	0.124	0.183	0.184
47	0.157	0.170	0.154	0.177	-	-	-	0.123	0.184	0.123	0.184	0.185
48	0.157	0.170	0.154	0.178	-	-	-	0.122	0.185	0.122	0.185	0.186
49	0.156	0.169	0.154	0.179	-	-	-	0.121	0.186	0.121	0.186	0.187
50	0.155	0.169	0.154	0.179	-	-	-	0.120	0.187	0.120	0.187	0.188
51	0.154	0.169	0.154	0.180	-	-	-	0.119	0.188	0.119	0.188	0.189
52	0.154	0.168	0.154	0.181	-	-	-	0.118	0.189	0.118	0.189	0.190
53	0.153	0.168	0.154	0.181	-	-	-	0.117	0.190	0.117	0.190	0.191
54	0.152	0.167	0.154	0.182	-	-	-	0.116	0.191	0.116	0.191	0.192
55	0.152	0.167	0.154	0.183	-	-	-	0.115	0.192	0.115	0.192	0.193
56	0.151	0.167	0.154	0.184	-	-	-	0.114	0.193	0.114	0.193	0.194
57	0.150	0.166	0.154	0.184	-	-	-	0.113	0.194	0.113	0.194	0.195
58	0.149	0.166	0.154	0.185	-	-	-	0.112	0.195	0.112	0.195	0.196
59	0.149	0.165	0.154	0.186	-	-	-	0.111	0.196	0.111	0.196	0.197
60	0.148	-	0.155	-	-	-	-	0.110	0.197	0.110	0.197	0.198

Table B.7: Einstein coefficients  $A$  of laser transitions of '838' CO<sub>2</sub>, s<sup>-1</sup>

$J$	Regular			Sequence			Hot-e			Hot-f		
	10P	10R	9P	9R	10P	10R	9P	9R	10P	10R	9P	9R
0	-	-	-	-	-	-	-	-	-	-	-	-
1	-	-	-	-	-	-	-	-	-	-	-	-
2	-	-	-	-	-	-	-	-	-	-	-	-
3	-	-	-	-	-	-	-	-	-	-	-	-
4	-	-	-	-	-	-	-	-	-	-	-	-
5	-	-	-	-	-	-	-	-	-	-	-	-
6	0.191	0.166	0.233	0.203	-	-	-	-	-	-	-	-
7	-	-	-	-	-	-	-	-	-	-	-	-
8	0.186	0.169	0.227	0.206	-	-	-	-	-	-	-	-
9	-	-	-	-	-	-	-	-	-	-	-	-
10	0.182	0.171	0.223	0.209	-	-	-	-	-	-	-	-
11	-	-	-	-	-	-	-	-	-	-	-	-
12	0.180	0.173	0.220	0.211	-	-	-	-	-	-	-	-
13	-	-	-	-	-	-	-	-	-	-	-	-
14	0.178	0.175	0.219	0.213	-	-	-	-	-	-	-	-
15	-	-	-	-	-	-	-	-	-	-	-	-
16	0.177	0.177	0.217	0.215	-	-	-	-	-	-	-	-
17	-	-	-	-	-	-	-	-	-	-	-	-
18	0.176	0.178	0.216	0.217	-	-	-	-	-	-	-	-
19	-	-	-	-	-	-	-	-	-	-	-	-
20	0.175	0.179	0.215	0.219	-	-	-	-	-	-	-	-
21	-	-	-	-	-	-	-	-	-	-	-	-
22	0.174	0.180	0.214	0.219	-	-	-	-	-	-	-	-
23	-	-	-	-	-	-	-	-	-	-	-	-
24	0.174	0.181	0.214	0.221	-	-	-	-	-	-	-	-
25	-	-	-	-	-	-	-	-	-	-	-	-
26	0.173	0.182	0.213	0.222	-	-	-	-	-	-	-	-
27	-	-	-	-	-	-	-	-	-	-	-	-
28	0.173	0.184	0.212	0.224	-	-	-	-	-	-	-	-
29	-	-	-	-	-	-	-	-	-	-	-	-
30	0.172	0.185	0.211	0.225	-	-	-	-	-	-	-	-
31	-	-	-	-	-	-	-	-	-	-	-	-
32	0.171	0.185	0.210	0.226	-	-	-	-	-	-	-	-
33	-	-	-	-	-	-	-	-	-	-	-	-
34	-	-	-	-	-	-	-	-	-	-	-	-
35	-	-	-	-	-	-	-	-	-	-	-	-
36	-	-	-	-	-	-	-	-	-	-	-	-
37	-	-	-	-	-	-	-	-	-	-	-	-
38	-	-	-	-	-	-	-	-	-	-	-	-
39	-	-	-	-	-	-	-	-	-	-	-	-
40	-	-	-	-	-	-	-	-	-	-	-	-
41	-	-	-	-	-	-	-	-	-	-	-	-
42	-	-	-	-	-	-	-	-	-	-	-	-
43	-	-	-	-	-	-	-	-	-	-	-	-
44	-	-	-	-	-	-	-	-	-	-	-	-
45	-	-	-	-	-	-	-	-	-	-	-	-
46	-	-	-	-	-	-	-	-	-	-	-	-
47	-	-	-	-	-	-	-	-	-	-	-	-
48	-	-	-	-	-	-	-	-	-	-	-	-
49	-	-	-	-	-	-	-	-	-	-	-	-
50	-	-	-	-	-	-	-	-	-	-	-	-
51	-	-	-	-	-	-	-	-	-	-	-	-
52	-	-	-	-	-	-	-	-	-	-	-	-
53	-	-	-	-	-	-	-	-	-	-	-	-
54	-	-	-	-	-	-	-	-	-	-	-	-
55	-	-	-	-	-	-	-	-	-	-	-	-
56	-	-	-	-	-	-	-	-	-	-	-	-
57	-	-	-	-	-	-	-	-	-	-	-	-
58	-	-	-	-	-	-	-	-	-	-	-	-
59	-	-	-	-	-	-	-	-	-	-	-	-
60	-	-	-	-	-	-	-	-	-	-	-	-

## Appendix C

# Properties of optical materials

The following expressions and values for linear ( $n_0$ ) and nonlinear ( $n_2$ ) refractive indexes and linear absorption ( $\alpha_0$ ) are used in the program (wavelength  $\lambda$  in the formulas must be expressed in  $\mu\text{m}$ ):

### Air

Refractive index  $n_0$  is calculated using Mathar's model for  $\lambda = 7.5\text{--}14\ \mu\text{m}$  [24]

$$n_2 = 3.0 \times 10^{-23}\ \text{m}^2/\text{W at } 9.2\ \mu\text{m} [25]$$

### AgBr

$$n_0 = \sqrt{3.860 + \frac{0.8677\lambda^2}{\lambda^2 - 0.3211^2} + \frac{21.61\lambda^2}{\lambda^2 - 254.2^2}}\ (\lambda = 0.495\text{--}12.67\ \mu\text{m}) [26]$$

$$n_2 = 6.0 \times 10^{-19}\ \text{m}^2/\text{W at } 9.2\ \mu\text{m} [26]$$

### AgCl

$$n_0 = \sqrt{4.00804 + \frac{0.079086}{\lambda^2 - 0.04584} - 0.00085111\lambda^2 - 0.00000019762\lambda^4}\ (\lambda = 0.578\text{--}20.6\ \mu\text{m}) [27]$$

$$n_2 = 4.8 \times 10^{-19}\ \text{m}^2/\text{W at } 9.2\ \mu\text{m} [26]$$

### BaF<sub>2</sub>

$$n_0 = \sqrt{1.33973 + \frac{0.81070\lambda^2}{\lambda^2 - 0.10065^2} + \frac{0.19652\lambda^2}{\lambda^2 - 29.87^2} + \frac{4.52469\lambda^2}{\lambda^2 - 53.82^2}}\ (\lambda = 0.15\text{--}15\ \mu\text{m}) [28]$$

$$n_2 = 1.7 \times 10^{-20}\ \text{m}^2/\text{W at } 9.2\ \mu\text{m} [29]$$

$$\alpha_0 = 0.8(e^{1.20(\lambda-8)} - 1)\ \text{m}^{-1} [26]$$

### CdTe

$$n_0 = \sqrt{1 + \frac{6.1977889\lambda^2}{\lambda^2 - 0.1005326} + \frac{3.2243821\lambda^2}{\lambda^2 - 5279.518}}\ (\lambda = 6\text{--}22\ \mu\text{m}) [30]$$

$$n_2 = -2.95 \times 10^{-17}\ \text{m}^2/\text{W at } 1.06\ \mu\text{m} [31]$$



## CsI

$$n_0 = \sqrt{1.27587 + \frac{0.68689\lambda^2}{\lambda^2-0.130^2} + \frac{0.26090\lambda^2}{\lambda^2-0.147^2} + \frac{0.06256\lambda^2}{\lambda^2-0.163^2} + \frac{0.06527\lambda^2}{\lambda^2-0.177^2} + \frac{0.14991\lambda^2}{\lambda^2-0.185^2} + \frac{0.51818\lambda^2}{\lambda^2-0.206^2} + \frac{0.01918\lambda^2}{\lambda^2-0.218^2} + \frac{3.38229\lambda^2}{\lambda^2-161.29^2}} \quad (\lambda = 0.25\text{--}67 \mu\text{m}) \quad [32]$$

$$n_2 = 1.2 \times 10^{-19} \text{ m}^2/\text{W at } 9.2 \mu\text{m} \quad [26]$$

## GaAs

$$n_0 = \sqrt{5.372514 + \frac{5.466742\lambda^2}{\lambda^2-0.4431307^2} + \frac{0.02429960\lambda^2}{\lambda^2-0.8746453^2} + \frac{1.957522\lambda^2}{\lambda^2-36.9166^2}} \quad (\lambda = 0.97\text{--}17 \mu\text{m}) \quad [33]$$

$$n_2 = 7.5 \times 10^{-18} \text{ m}^2/\text{W at } 9.2 \mu\text{m} \quad [26]$$

## Ge

$$n_0 = \sqrt{1 + \frac{0.4886331\lambda^2}{\lambda^2-1.393959} + \frac{14.5142535\lambda^2}{\lambda^2-0.1626427} + \frac{0.0091224\lambda^2}{\lambda^2-752.190}} \quad (\lambda = 2\text{--}14 \mu\text{m}) \quad [34]$$

$$n_2 = 4.0 \times 10^{-17} \text{ m}^2/\text{W at } 9.2 \mu\text{m} \quad [26]$$

## IRG22 (AMTIR1)

$$n_0 = \sqrt{3.4834 + \frac{2.8203\lambda^2}{\lambda^2-0.1352} + \frac{0.9773\lambda^2}{\lambda^2-1420.7}} \quad (\lambda = 0.8\text{--}15.5 \mu\text{m}) \quad [35]$$

$$n_2 = 1.4 \times 10^{-18} \text{ m}^2/\text{W at } 9.2 \mu\text{m} \quad [26]$$

## IRG24

$$n_0 = \sqrt{3.8965 + \frac{2.9567\lambda^2}{\lambda^2-0.1620} + \frac{0.9461\lambda^2}{\lambda^2-1939.1}} \quad (\lambda = 0.8\text{--}15.5 \mu\text{m}) \quad [36]$$

$$n_2 = 2.5 \times 10^{-18} \text{ m}^2/\text{W at } 9.2 \mu\text{m} \quad [26]$$

## IRG25

$$n_0 = \sqrt{3.7574 + \frac{3.0990\lambda^2}{\lambda^2-0.1596} + \frac{1.6660\lambda^2}{\lambda^2-2045.5}} \quad (\lambda = 0.8\text{--}15.5 \mu\text{m}) \quad [37]$$

$$n_2 = 2.3 \times 10^{-18} \text{ m}^2/\text{W at } 9.2 \mu\text{m} \quad [26]$$

## KBr

$$n_0 = \sqrt{1.39408 + \frac{0.79221\lambda^2}{\lambda^2-0.146^2} + \frac{0.01981\lambda^2}{\lambda^2-0.173^2} + \frac{0.15587\lambda^2}{\lambda^2-0.187^2} + \frac{0.17673\lambda^2}{\lambda^2-60.61^2} + \frac{2.06217\lambda^2}{\lambda^2-87.72^2}} \quad (\lambda = 0.2\text{--}42 \mu\text{m}) \quad [32]$$

$$n_2 = 4.3 \times 10^{-20} \text{ m}^2/\text{W at } 9.2 \mu\text{m} \quad [26]$$

## KCl

$$n_0 = \sqrt{1.26486 + \frac{0.30523\lambda^2}{\lambda^2-0.100^2} + \frac{0.41620\lambda^2}{\lambda^2-0.131^2} + \frac{0.18870\lambda^2}{\lambda^2-0.162^2} + \frac{2.6200\lambda^2}{\lambda^2-70.42^2}} \quad (\lambda = 0.18\text{--}35 \mu\text{m}) \quad [32]$$

$$n_2 = 3.4 \times 10^{-20} \text{ m}^2/\text{W at } 9.2 \mu\text{m} \quad [29]$$

## KRS5

$$n_0 = \sqrt{1 + \frac{1.8293958\lambda^2}{\lambda^2 - 0.0225} + \frac{1.6675593\lambda^2}{\lambda^2 - 0.0625} + \frac{1.1210424\lambda^2}{\lambda^2 - 0.1225} + \frac{0.04513366\lambda^2}{\lambda^2 - 0.2025} + \frac{12.380234\lambda^2}{\lambda^2 - 27089.737}} \quad (\lambda = 0.577\text{--}39.4\text{ }\mu\text{m}) \quad [38]$$

$$n_2 = 9.0 \times 10^{-19} \text{ m}^2/\text{W at } 9.2\text{ }\mu\text{m} \quad [26]$$

## NaCl

$$n_0 = \sqrt{1.00055 + \frac{0.19800\lambda^2}{\lambda^2 - 0.050^2} + \frac{0.48398\lambda^2}{\lambda^2 - 0.100^2} + \frac{0.38696\lambda^2}{\lambda^2 - 0.128^2} + \frac{0.25998\lambda^2}{\lambda^2 - 0.158^2} + \frac{0.08796\lambda^2}{\lambda^2 - 40.50^2} + \frac{3.17064\lambda^2}{\lambda^2 - 60.98^2} + \frac{0.30038\lambda^2}{\lambda^2 - 120.34^2}} \quad (\lambda = 0.2\text{--}30\text{ }\mu\text{m}) \quad [32]$$

$$n_2 = 3.5 \times 10^{-20} \text{ m}^2/\text{W at } 9.2\text{ }\mu\text{m} \quad [29]$$

## NaF

$$n_0 = \sqrt{1.41572 + \frac{0.32785\lambda^2}{\lambda^2 - 0.117^2} + \frac{3.18248\lambda^2}{\lambda^2 - 40.57^2}} \quad (\lambda = 0.15\text{--}17\text{ }\mu\text{m}) \quad [32]$$

$$n_2 = 6.0 \times 10^{-21} \text{ m}^2/\text{W at } 9.2\text{ }\mu\text{m} \quad [26]$$

$$\alpha_0 = 5.0(e^{0.97(\lambda-8)} - 1) \text{ m}^{-1} \quad [26]$$

## Si

$$n_0 = 3.41983 + \frac{0.159906}{\lambda^2 - 0.028} - 0.123109 \left( \frac{1}{\lambda^2 - 0.028} \right)^2 + 1.26878 \times 10^{-6} \lambda^2 - 1.95104 \times 10^{-9} \lambda^4 \quad (\lambda = 2.44\text{--}25\text{ }\mu\text{m}) \quad [39]$$

$$n_2 = 1.2 \times 10^{-17} \text{ m}^2/\text{W at } 9.2\text{ }\mu\text{m} \quad [26]$$

## SiO<sub>2</sub>

$$n_0 = \sqrt{1 + \frac{0.6961663\lambda^2}{\lambda^2 - 0.0684043^2} + \frac{0.4079426\lambda^2}{\lambda^2 - 0.1162414^2} + \frac{0.8974794\lambda^2}{\lambda^2 - 9.896161^2}} \quad (\lambda = 0.21\text{--}6.7\text{ }\mu\text{m}) \quad [40]$$

$$n_2 = 3.29 \times 10^{-20} \text{ m}^2/\text{W at } 1.06\text{ }\mu\text{m} \quad [31]$$

## ZnS

$$n_0 = \sqrt{8.393 + \frac{0.14383}{\lambda^2 - 0.2421^2} + \frac{4430.99}{\lambda^2 - 36.71^2}} \quad (\lambda = 0.405\text{--}13\text{ }\mu\text{m}) \quad [41]$$

$$n_2 = 4.0 \times 10^{-19} \text{ m}^2/\text{W at } 9.2\text{ }\mu\text{m} \quad [26]$$

## ZnSe

$$n_0 = \sqrt{1 + \frac{4.45813734\lambda^2}{\lambda^2 - 0.200859853^2} + \frac{0.467216334\lambda^2}{\lambda^2 - 0.391371166^2} + \frac{2.89566290\lambda^2}{\lambda^2 - 47.1362108^2}} \quad (\lambda = 0.54\text{--}18.2\text{ }\mu\text{m}) \quad [42]$$

$$n_2 = 6.5 \times 10^{-19} \text{ m}^2/\text{W at } 9.2\text{ }\mu\text{m} \quad [26]$$

## Appendix D

# Selected formulas explained

### Equation 4.4

Eq. 4.4 defines the fraction  $z_{jk}$  of discharge energy spent in inelastic collisions:

$$z_{jk} = 10^{16} \frac{y_j u_{jk} \omega_{jk}}{\left( \frac{\xi \mathcal{E}}{\mathcal{N}} \right) v_d}$$

where  $y_j[-]$  is the relative concentration of a component in the gas mixture,  $u_{jk}[\text{eV}]$  is the transferred energy per electron-molecule collision, collision rate constant  $\omega_{jk}[\text{cm}^3 \cdot \text{s}^{-1}]$  divided by electron drift speed  $v_d[\text{cm} \cdot \text{s}^{-1}]$  is the collision cross-section ( $[\text{cm}^2]$ ),  $\mathcal{E}[10^{-16} \text{V} \cdot \text{cm}^{-1}]$  is the electric field,  $\xi[\text{eV} \cdot \text{V}^{-1}]$  is the energy gained by electron moved across an electric potential difference of 1 V, and  $\mathcal{N}[\text{cm}^{-3}]$  is the total absolute concentration of the gas mixture.

The physical meaning of  $\xi \mathcal{E}$  is the energy (in eV) gained by an electron after passing 1 cm in the electric field  $\mathcal{E}$ . By definition of electronvolt,  $\xi = 1$  and is thus omitted in Eq. 4.4.

### Pumping rate constants in equations 4.8 and 4.9

Pumping rate constant is the number of quanta added to a given vibrational mode per unit of time per molecule.

$$p_e = \frac{1}{E_v[\text{J}]} \times \frac{1}{N[\text{cm}^{-3}]n[-]y[-]} \times q[-]W[\text{J} \cdot \text{s}^{-1} \cdot \text{cm}^{-3}]$$

where  $E_v$  is the energy of the vibrational quanta: 4.665e-20 J (2349  $\text{cm}^{-1}$ ) for  $\nu_3$  mode of  $\text{CO}_2$  (and roughly same for  $\text{N}_2$  vibration), and 1.325e-20 J (667  $\text{cm}^{-1}$ ) for  $\nu_2$  mode;  $N=2.7\text{e}19 \text{ cm}^{-3}$  is the density of gas molecules under normal conditions (1 bar, 273 K);  $q$  is the fraction of discharge energy deposited in the corresponding vibration;  $n$  is the correction factor for molecular density at the conditions different from 'normal';  $y$  is the relative concentration of the gas in the mixture;  $W$  is the discharge power density.

Combining the constants and switching to  $\text{kW}/\text{cm}^3$  for power density and  $\mu\text{s}^{-1}$  for the rate constants we get the formulas given in the model description:

$$p_{e4} = 0.8 \times 10^{-3} \frac{q_4}{ny_2} W(t); \quad p_{e3} = 0.8 \times 10^{-3} \frac{q_3}{ny_1} W(t); \quad p_{e2} = 2.8 \times 10^{-3} \frac{q_2}{ny_1} W(t);$$

# Bibliography

- [1] M. Born and E. Wolf, *Principles of Optics: Electromagnetic Theory of Propagation, Interference and Diffraction of Light*. Cambridge University Press, 1999.
- [2] A. E. Siegman, *Lasers*. University Science Books, 1986.
- [3] J. Peatross and M. Ware, *Physics of Light and Optics*. Available at optics.byu.edu, 2015.
- [4] N. V. Karlov and Y. B. Konev, “High pressure pulsed CO<sub>2</sub> lasers,” in *Handbook on lasers*, A. M. Prokhorov, Ed., In Russian, Moscow: Sovetskoe Radio, 1978.
- [5] T. Holstein, “Energy distribution of electrons in high frequency gas discharges,” *Phys. Rev.*, vol. 70, pp. 367–384, 1946. DOI: 10.1103/PhysRev.70.367.
- [6] W. L. Nighan, “Electron energy distributions and collision rates in electrically excited N<sub>2</sub>, CO, and CO<sub>2</sub>,” *Phys. Rev. A*, vol. 2, pp. 1989–2000, 1970. DOI: 10.1103/PhysRevA.2.1989.
- [7] R. D. Hake and A. V. Phelps, “Momentum-transfer and inelastic-collision cross sections for electrons in O<sub>2</sub>, CO, and CO<sub>2</sub>,” *Phys. Rev.*, vol. 158, pp. 70–84, 1967. DOI: 10.1103/PhysRev.158.70.
- [8] L. S. Frost and A. V. Phelps, “Rotational excitation and momentum transfer cross sections for electrons in H<sub>2</sub> and N<sub>2</sub> from transport coefficients,” *Phys. Rev.*, vol. 127, pp. 1621–1633, 1962. DOI: 10.1103/PhysRev.127.1621.
- [9] A. S. Biryukov, V. K. Konyukhov, A. I. Lukovnikov, and R. I. Serikov, “Relaxation of the vibrational energy of the (00<sup>0</sup>1) level of the CO<sub>2</sub> molecule,” *Sov. J. Exp. Theor. Phys.*, vol. 39, p. 610, 1974.
- [10] R. L. Taylor and S. Bitterman, “Survey of vibrational relaxation data for processes important in the CO<sub>2</sub>-N<sub>2</sub> laser system,” *Rev. Mod. Phys.*, vol. 41, pp. 26–47, 1969. DOI: 10.1103/RevModPhys.41.26.
- [11] B. J. Feldman, “Short-pulse multiline and multiband energy extraction in high-pressure CO<sub>2</sub>-laser amplifiers,” *IEEE J. Quant. Electron.*, vol. 9, pp. 1070–1078, 1973. DOI: 10.1109/JQE.1973.1077412.
- [12] H. C. Volkin, “Calculation of short-pulse propagation in a large CO<sub>2</sub>-laser amplifier,” *J. Appl. Phys.*, vol. 50, pp. 1179–1188, 1979. DOI: 10.1063/1.326148.
- [13] R. C. Hilborn, “Einstein coefficients, cross sections, f values, dipole moments, and all that,” *arXiv:physics/0202029*, 2002.
- [14] W. J. Witteman, *The CO<sub>2</sub> Laser*. Berlin Heidelberg New York Tokyo: Springer-Verlag, 1987.
- [15] J. J. Lowke, A. V. Phelps, and B. W. Irwin, “Predicted electron transport coefficients and operating characteristics of CO<sub>2</sub>-N<sub>2</sub>-He laser mixtures,” *J. Appl. Phys.*, vol. 44, pp. 4664–4671, 1973. DOI: 10.1063/1.1662017.
- [16] Y. D. Oksyuk, “Excitation of the rotational levels of diatomic molecules by electron impact in the adiabatic approximation,” *Sov. J. Exp. Theor. Phys.*, vol. 22, pp. 873–881, 1966.
- [17] N. Chandra and P. G. Burke, “Rotational excitation cross sections for e<sup>−</sup>-N<sub>2</sub> scattering,” *J. Phys. B: At. Mol. Phys.*, vol. 6, pp. 2355–2357, 1973. DOI: 10.1088/0022-3700/6/11/030.
- [18] A. V. Phelps, “Rotational and vibrational excitation of molecules by low-energy electrons,” *Rev. Mod. Phys.*, vol. 40, pp. 399–410, 1968. DOI: 10.1103/RevModPhys.40.399.

- [19] G. J. Schulz, “Vibrational excitation of nitrogen by electron impact,” *Phys. Rev.*, vol. 125, pp. 229–232, 1962. DOI: 10.1103/PhysRev.125.229.
- [20] A. G. Engelhardt, A. V. Phelps, and C. G. Risk, “Determination of momentum transfer and inelastic collision cross sections for electrons in nitrogen using transport coefficients,” *Phys. Rev.*, vol. 135, A1566–A1574, 1964. DOI: 10.1103/PhysRev.135.A1566.
- [21] I. E. Gordon *et al.*, “The hitran2016 molecular spectroscopic database,” *J. Quant. Spectr. Rad. Transfer*, vol. 203, pp. 3–69, 2017. DOI: 10.1016/j.jqsrt.2017.06.038.
- [22] A. Maki, C. Chou, K. Evenson, L. Zink, and J. Shy, “Improved molecular constants and frequencies for the CO<sub>2</sub> laser from new high-j regular and hot-band frequency measurements,” *J. Mol. Spectr.*, vol. 167, pp. 211–224, 1994. DOI: 10.1006/jmsp.1994.1227.
- [23] C. Freed, “Status of CO<sub>2</sub> isotope lasers and their applications in tunable laser spectroscopy,” *IEEE J. Quant. Electron.*, vol. 18, pp. 1220–1228, 1982. DOI: 10.1109/JQE.1982.1071680.
- [24] R. J. Mathar, “Refractive index of humid air in the infrared: Model fits,” *J. Opt. A*, vol. 9, pp. 470–476, 2007. DOI: 10.1088/1464-4258/9/5/008.
- [25] M. N. Polyanskiy, M. Babzien, I. V. Pogorelsky, R. Kupfer, K. L. Vodopyanov, and M. A. Palmer, “Single-shot measurement of the nonlinear refractive index of air at 92  $\mu\text{m}$  with a picosecond terawatt CO<sub>2</sub> laser,” *Opt. Lett.*, vol. 46, p. 2067, 2021. DOI: 10.1364/ol.423800.
- [26] M. Polyanskiy, I. Pogorelsky, M. Babzien, K. Vodopyanov, and M. Palmer, “Nonlinear refraction and absorption properties of optical materials for high-peak-power long-wave-infrared lasers,” Nov. 2023. DOI: 10.1364/opticaopen.24615624. [Online]. Available: <http://dx.doi.org/10.1364/opticaopen.24615624>.
- [27] L. W. Tilton, E. K. Plyler, and R. E. Stephens, “Refractive index of silver chloride for visible and infra-red radiant energy,” *J. Opt. Soc. Am.*, vol. 40, p. 540, 1950. DOI: 10.1364/josa.40.000540.
- [28] H. H. Li, “Refractive index of alkaline earth halides and its wavelength and temperature derivatives,” *J. Phys. Chem. Ref. Data*, vol. 9, pp. 161–290, 1980. DOI: 10.1063/1.555616.
- [29] M. N. Polyanskiy, I. V. Pogorelsky, M. Babzien, R. Kupfer, K. L. Vodopyanov, and M. A. Palmer, “Post-compression of long-wave infrared 2 picosecond sub-terawatt pulses in bulk materials,” *Opt. Express*, vol. 29, no. 20, p. 31 714, 2021. DOI: 10.1364/oe.434238.
- [30] A. G. DeBell, E. L. Dereniak, J. Harvey, J. P. J. Nissley, A. Selvarajan, and W. L. Wolfe, “Cryogenic refractive indices and temperature coefficients of cadmium telluride from 6  $\mu\text{m}$  to 22  $\mu\text{m}$ ,” *Appl. Opt.*, vol. 18, pp. 3114–3115, 1979. DOI: 10.1364/AO.18.003114.
- [31] M. Sheik-Bahae, “Dispersion of bound electron nonlinear refraction in solids,” *IEEE J. Quant. Electron.*, vol. 27, pp. 1296–1309, 1991. DOI: 10.1109/3.89946.
- [32] H. H. Li, “Refractive index of alkali halides and its wavelength and temperature derivatives,” *J. Phys. Chem. Ref. Data*, vol. 5, pp. 329–528, 1976. DOI: 10.1063/1.555536.
- [33] T. Skauli *et al.*, “Improved dispersion relations for GaAs and applications to nonlinear optics,” *J. Appl. Opt.*, vol. 94, pp. 6447–6455, 2003. DOI: 10.1063/1.1621740.
- [34] J. H. Burnett, S. G. Kaplan, E. Stover, and A. Phenis, “Refractive index measurements of ge,” P. D. LeVan, A. K. Sood, P. Wijewarnasuriya, and A. I. D’Souza, Eds., SPIE Optical Engineering + Applications, 2016, San Diego, California, United States, SPIE, 2016. DOI: 10.1117/12.2237978.
- [35] *SCHOTT IRG 22 product flyer*, Apr. 2017. [Online]. Available: <https://refractiveindex.info/download/data/2017/schott-infrared-chalcogenide-glasses-irg-22-english-us-11052017.pdf>.
- [36] *SCHOTT IRG 24 product flyer*, Apr. 2017. [Online]. Available: <https://refractiveindex.info/download/data/2017/schott-infrared-chalcogenide-glasses-irg-24-english-us-10042017.pdf>.

- [37] *SCHOTT IRG 25 product flyer*, Apr. 2017. [Online]. Available: <https://refractiveindex.info/download/data/2017/schott-infrared-chalcogenide-glasses-irg-25-english-us-10042017.pdf>.
- [38] W. S. Rodney and I. H. Malitson, "Refraction and dispersion of thallium bromide iodide," *Journal of the Optical Society of America*, vol. 46, no. 11, p. 956, 1956. DOI: 10.1364/josa.46.000956. [Online]. Available: <https://doi.org/10.1364/josa.46.000956>.
- [39] D. F. Edwards and E. Ochoa, "Infrared refractive index of silicon," *Appl. Opt.*, vol. 19, pp. 4130–4131, 1980. DOI: 10.1364/AO.19.004130.
- [40] I. H. Malitson, "Interspecimen comparison of the refractive index of fused silica," *J. Opt. Soc. Am.*, vol. 55, p. 1205, Oct. 1965. DOI: 10.1364/josa.55.001205.
- [41] C. A. Klein, "Room-temperature dispersion equations for cubic zinc sulfide," *Appl. Opt.*, vol. 25, p. 1873, 1986. DOI: 10.1364/ao.25.001873.
- [42] B. Tatian, "Fitting refractive-index data with the Sellmeier dispersion formula," *Appl. Opt.*, vol. 23, pp. 4477–4485, 1984. DOI: 10.1364/AO.23.004477.